REGISTERED No. M. 3121

UNIVERSITY OF MICHIGAN
FEB 4 1960
PHYSICS LIBRARY

PROCEEDINGS

OF THE

INDIAN ACADEMY OF SCIENCES

VOL. L] SECTION A [No. 5

NOVEMBER 1959

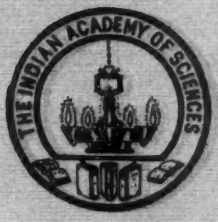

Price Rs. 2 or 3 Sh. *Annual Subscription Rs. 18*

PRINTED AT THE BANGALORE PRESS, BANGALORE CITY, BY C. VASUDEVA RAO, SUPERINTENDENT, AND PUBLISHED BY THE INDIAN ACADEMY OF SCIENCES, BANGALORE.

THE DIFFRACTION OF LIGHT BY TWO SUPERPOSED PARALLEL SUPERSONIC WAVES BEING HARMONICS OF THE SAME FUNDAMENTAL

By Robert Mertens*

(Rijksuniversiteit Gent, Seminarie voor Wiskundige Natuurkunde, Ghent, Belgium)

Received August 19, 1959

(Communicated by Sir C. V. Raman, F.R.S., N.L.)

1. Introduction

The theory of the diffraction of light by two superposed parallel supersonic waves, the frequency of one of them being a multiple of the frequency of the other, has been investigated by Ramachandra Rao[1] and Murty[2] using the methods of Raman and Nath's preliminary theory.[3] Employing the reasoning of Raman and Nath's generalized theory,[4] Zankel and Hiedemann[5] and Mertens[6] extended those calculations, starting from the wave equation for the electric field of the light.

Other theories, mainly based on Raman and Nath's preliminary theory, were developed by Bergmann and Fues,[7] Nagendra Nath[8] and Nagabhushana Rao[9] for sound waves with incommensurate frequencies and presenting no phase differences.

In the present paper we shall expose the general theory of the diffraction of light by two superposed parallel supersonic waves having arbitrary frequencies. We shall, however, suppose that the ratio of those frequencies ν_1^* and ν_2^* is equal to the ratio of two simple incommensurable integers n_1 and n_2, different from one. This problem will be encountered experimentally when the piezo-electric crystal generating the supersonic waves is excited at two harmonics (the fundamental tone being excluded), the frequency of one of them being no multiple of the frequency of the other. To our knowledge the only experimental treatment of such a case was given by Bergmann,[10] who observed orders corresponding to $\nu_1^* \pm \nu_2^*$, ν_1^* and ν_2^*. In the following section a system of difference-differential equations for the amplitudes of the different orders is derived. In § 3 the special case of very intense supersonic waves of large wavelengths is considered and the corresponding system of difference-differential equations is solved exactly. Finally

* Geassocieerde van het Nationaal Fonds voor Wetenschappelijk Onderzoek van België.

in the last section the conditions for the asymmetry of the diffraction pattern with respect to the zero order are derived.

2. A System of Difference-Differential Equations for the Amplitudes of the Diffracted Light Waves

As usual let us consider a parallel beam of monochromatic light of frequency ν and wavelength in vacuum λ, passing through a liquid column. The liquid is disturbed by two superposed parallel progressive supersonic waves, the ratio of the frequencies of which is $\nu_1^*/\nu_2^* = n_1/n_2$, where n_1 and n_2 are simple incommensurable integers, the case, n_1 or n_2 equal to one, already treated in an earlier paper,[6] being excluded. We shall suppose that the directions of propagation of the incident light and the sound waves are perpendicular to each other, We shall further put the z-axis along the direction of the incident light and the x-axis along the direction of the sound waves.

Following the method of Raman and Nath's generalized theory[4] for one ultrasonic wave, the electric field of the light may be written

$$E(x, z, t) = e^{2\pi i\nu t}\phi(x, z, t), \tag{1}$$

$\phi(x, z, t)$ satisfying the equation

$$\Delta\phi = -\left(\frac{2\pi}{\lambda}\right)^2 \mu^2(x, t)\,\phi; \tag{2}$$

$\mu(x, t)$ is the refractive index of the disturbed liquid and is given by the expression

$$\mu(x, t) = \mu_0 + \mu_1 \sin 2\pi\left(\nu_1^* t - \frac{x}{\lambda_1^*} + \Delta_1\right) + \mu_2 \sin 2\pi\left(\nu_2^* t - \frac{x}{\lambda_2^*} + \Delta_2\right), \tag{3}$$

where

λ_1^*, λ_2^* = wavelengths of the supersonic waves in the medium;

ν_1^*, ν_2^* = frequencies of the supersonic waves;

μ_0 = refractive index of the undisturbed medium;

μ_1, μ_2 = maximum variation of the refractive index of the disturbed medium, due to each of the supersonic waves;

Δ_1, Δ_2 = phase constants of the supersonic waves.

Let Λ be the least common multiple of λ_1^* and λ_2^*, so we have

$$\Lambda = n_1\lambda_1^* = n_2\lambda_2^*. \tag{4}$$

According to the formulæ

$$\nu_1^* = \frac{c^*}{\lambda_1^*} = \frac{c^* n_1}{\Lambda}, \quad \nu_2^* = \frac{c^*}{\lambda_2^*} = \frac{c^* n_2}{\Lambda}$$

where c^* is the velocity of propagation of the supersonic waves in the liquid, and putting $N = c^*/\Lambda$ we obtain

$$\nu_1^* = n_1 N, \quad \nu_2^* = n_2 N$$

or

$$\frac{1}{N} = \frac{n_1}{\nu_1^*} = \frac{n_2}{\nu_2^*}. \tag{5}$$

From the formula (3) for the refractive index and taking (4) and (5) into account, it is clear that the following periodicity conditions are valid,

$$\mu(x + p\Lambda, t) = \mu(x + pn_1\lambda_1^*, t) = \mu(x + pn_2\lambda_2^*, t) = \mu(x, t), \tag{6 a}$$

$$\mu\left(x, t + \frac{p}{N}\right) = \mu\left(x, t + \frac{pn_1}{\nu_1^*}\right) = \mu\left(x, t + \frac{pn_2}{\nu_2^*}\right) = \mu(x, t), \tag{6 b}$$

p being an integer. Hence, the following conditions hold for the function $\phi(x, z, t)$

$$\phi(x + p\Lambda, z, t) = \phi(x, z, t), \tag{7 a}$$

$$\phi\left(x, z, t + \frac{p}{N}\right) = \phi(x, z, t). \tag{7 b}$$

Further we have also the condition, expressing that the sound wave is a progressive one,

$$\mu(x + \rho\Lambda, z, t) = \mu\left(x, z, t - \frac{\rho}{N}\right), \tag{8}$$

ρ being an arbitrary number, leading to

$$\phi(x + \rho\Lambda, z, t) = \phi\left(x, z, t - \frac{\rho}{N}\right). \tag{9}$$

With regard to the periodicity of $\phi(x, z, t)$ in x and t, expressed by (7 *a*, *b*), this function may be developed in a double Fourier series, which, taking into account the condition (9), may be written in the following form,

$$\phi(x, z, t) = \sum_{n=-\infty}^{\infty} f_n(z)\, e^{2\pi i n x/\Lambda}\, e^{-2\pi i n N t}. \tag{10}$$

Substituting this series and the expression (3) for the refractive index into the differential equation (2), neglecting the terms in μ_1^2, μ_2^2 and $\mu_1\mu_2$ with respect to those in μ_1 and μ_2, and equating the coefficients of

$$\exp 2\pi i n \frac{x}{\Lambda} \cdot \exp - 2\pi i n N t$$

on both sides, we obtain

$$-\frac{4\pi^2}{\Lambda^2} f_n(z)\, n^2 + \frac{d^2 f_n}{dz^2} = -\frac{4\pi^2\mu_0^2}{\lambda^2} f_n$$
$$-\frac{8\pi^2\mu_0\mu_1}{2i\lambda^2}\left\{ f_{n+n_1} e^{2\pi i \Delta_1} - f_{n-n_1} e^{-2\pi i \Delta_1}\right\}$$
$$-\frac{8\pi^2\mu_0\mu_2}{2i\lambda^2}\left\{ f_{n+n_2} e^{2\pi i \Delta_2} - f_{n-n_2} e^{-2\pi i \Delta_2}\right\}.$$

Putting further

$$f_n(z) = \exp\left(-i\frac{2\pi}{\lambda}\mu_0 z\right)\phi_n(z)$$

and neglecting the term in $d^2\phi_n/dz^2$ with respect to the others, the following system of difference-differential equations for the coefficients $\phi_n(z)$ may be written,

$$2\frac{d\phi_n}{dz} - \sigma_1\{\phi_{n-n_1} e^{-i\delta_1} - \phi_{n+n_1} e^{i\delta_1}\} - \sigma_2\{\phi_{n-n_2} e^{-i\delta_2} - \phi_{n+n_2} e^{i\delta_2}\}$$
$$= i\beta n^2 \phi_n \tag{11}$$

with

$$\sigma_i = \frac{2\pi\mu_i}{\lambda}, \quad \beta = \frac{2\pi\lambda}{\mu_0\Lambda^2}, \quad \delta_i = 2\pi\Delta_i \quad (i = 1, 2). \tag{12}$$

From (10) it is seen that the spectrum of order n makes an angle with the z-axis, defined by

$$\sin\theta_n = -n\frac{\lambda}{\Lambda}. \tag{13}$$

We now remark that it is possible to write in an indefinite number of ways that $n = rn_1 + sn_2$, whereby r and s are couples of integers between $-\infty$ and $+\infty$. Hence,

$$\sin\theta_n = -n\frac{\lambda}{\Lambda} = -rn_1\frac{\lambda}{\Lambda} - sn_2\frac{\lambda}{\Lambda} = -\left(r\frac{\lambda}{\lambda_1^*} + s\frac{\lambda}{\lambda_2^*}\right) = \sin\theta_{rs}, \tag{14}$$

where use has been made of the relations (4).

Again from formula (10) follows that the n-th order spectrum undergoes a frequency change $-nN$, which becomes if we take formula (5) into account,

$$-nN = -(rn_1 + sn_2)N = -(r\nu_1^* + s\nu_2^*). \tag{15}$$

We may thus conclude that the n-th order can be considered as a superposition of partial orders (r, s), where r and s are all couples of integers satisfying the relation $n = rn_1 + sn_2$.

The n-th order amplitude ϕ_n may be decomposed into a sum of partial amplitudes of order (r, s),

$$\phi_n = \sum_{r,s} \phi_{rs}, \tag{16}$$

where the summation is performed over all couples of integers r, s obeying the relation $n = rn_1 + sn_2$.

The system (11) may further be simplified by eliminating one of the phase constants. Therefore we shall put

$$\phi_n = \psi_n \, e^{in\delta_1/n_1} \tag{17}$$

into the equation (11); putting $\delta = (n_1\delta_2 - n_2\delta_1)/n_1$ we obtain

$$2\frac{d\psi_n}{dz} - \sigma_1(\psi_{n-n_1} - \psi_{n+n_1}) - \sigma_2\{\psi_{n-n_2}e^{-i\delta} - \psi_{n+n_2}e^{i\delta}\} = i\beta n^2\psi_n. \tag{18}$$

We could, of course, have written this equation directly by introducing $\delta_1 = 0$ and $\delta_2 = \delta$ in the expression for the refractive index.†

Let further be

$$\zeta = \frac{2\pi\mu}{\lambda} z = \sigma_1 z, \quad a = \frac{\sigma_2}{\sigma_1} = \frac{\mu_2}{\mu_1}, \quad \rho_1 = \frac{\beta}{\sigma_1} = \frac{\lambda^2}{\mu_0\mu_1\Lambda^2}, \tag{19}$$

then the system (18) becomes finally

$$\boxed{2\frac{d\psi_n}{d\zeta} - (\psi_{n-n_1} - \psi_{n+n_1}) - a\{\psi_{n-n_2}e^{-i\delta} - \psi_{n+n_2}e^{i\delta}\} = i\rho_1 n^2\psi_n} \tag{20}$$

The solutions of this infinite system of difference-differential equations satisfying the boundary conditions

$$\psi_n(0) = \delta_{n0} \tag{21}$$

(δ_{n0} being the well-known Kronecker symbol), are the amplitudes of the diffracted orders, a complex factor of modulus one excepted.

† We have the same situation in the case of one progressive supersonic wave, when the refractive index is given by $\mu(x, t) = \mu_0 + \mu_1 \sin 2\pi(\nu^* t - x/\lambda^* + \Delta)$. The generalized theory of Raman and Nath then leads to the system

$$2\frac{d\phi_n}{d\xi} - \{\phi_{n-1}e^{-i\delta} - \phi_{n+1}e^{i\delta}\} = i\rho n^2\phi_n$$

with

$$\xi = \frac{2\pi u_1 z}{\lambda}, \quad \rho = \frac{\lambda^2}{\mu_0\mu_1\lambda^{*2}} \text{ and } \delta = 2\pi\Delta;$$

the substitution $\phi_n = \psi_n e^{-in\delta}$ transforms the system into

$$2\frac{d\psi_n}{d\xi} - (\psi_{n-1} - \psi_{n+1}) = i\rho n^2\psi_n$$

which is the usual Raman-Nath system without a phase constant.

3. SPECIAL CASE: $\rho_1 = 0$

For great values of μ_1 and Λ, *i.e.*, great values of both supersonic wavelengths λ_1^* and λ_2^*, ρ_1 becomes approximately zero, so that the r.h.s. of equation (20) is negligible. The system now takes the form

$$2\frac{d\psi_n}{d\zeta} - (\psi_{n-n_1} - \psi_{n+n_1}) - \alpha\{\psi_{n-n_2}e^{-i\delta} - \psi_{n+n_2}e^{i\delta}\} = 0, \tag{22}$$

with the same boundary conditions (21), and we shall prove that it may be integrated exactly. Therefore we shall follow the complex function method of Nagendra Nath-Wilson.[8] We put

$$\psi_n(\zeta) = \frac{1}{2\pi i}\oint F(\eta)\frac{e^{\zeta f(\eta)}}{\eta^{n+1}}\,d\eta, \tag{23}$$

where $F(\eta)$ and $f(\eta)$ are yet unknown functions of the complex variable η and the integral is taken along a closed path in the complex η-plane encircling the origin once in the positive sence. The boundary conditions (21) require that

$$F(\eta) = 1. \tag{24}$$

Substitution of the solution (23) into the equation (22) leads to the determination of the function $f(\eta)$,

$$f(\eta) = \frac{1}{2}\left(\eta^{n_1} - \frac{1}{\eta^{n_1}}\right) + \frac{\alpha}{2}\left\{\eta^{n_2}e^{-i\delta} - \frac{1}{\eta^{n_2}e^{-i\delta}}\right\} \tag{25}$$

so that (23) may be written

$$\psi_n(\zeta) = \frac{1}{2\pi i}\oint \frac{\exp\left[\frac{\zeta}{2}\left(\eta^{n_1} - \frac{1}{\eta^{n_1}}\right)\right]\exp\left[\frac{\alpha\zeta}{2}\left(\eta^{n_2}e^{-i\delta} - \frac{1}{\eta^{n_2}e^{-i\delta}}\right)\right]}{\eta^{n+1}}\,d\eta. \tag{26}$$

The exponential functions in the integrand may be developed in the well-known Laurent expansions,[11]

$$\exp\frac{\zeta}{2}\left(\eta^{n_1} - \frac{1}{\eta^{n_1}}\right) = \sum_{r=-\infty}^{\infty} J_r(\zeta)\,\eta^{n_1 r}, \tag{27 a}$$

$$\exp\frac{\alpha\zeta}{2}\left(\eta^{n_2}e^{-i\delta} - \frac{1}{\eta^{n_2}e^{-i\delta}}\right) = \sum_{s=-\infty}^{\infty} J_s(\alpha\zeta)\,\eta^{n_2 s}e^{-is\delta}, \tag{27 b}$$

where $J_n(z)$ denotes the Bessel function of order n. Substituting those series into the r.h.s. of (26) we get

$$\psi_n(\zeta) = \frac{1}{2\pi i} \sum_{r,s=-\infty}^{\infty} J_r(\zeta)\, J_s(a\zeta)\, e^{-is\delta} \oint \eta^{n_1 r + n_2 s - n - 1} d\eta.$$

The integral having the value $2\pi i \delta_{n, n_1 r + n_2 s}$ we obtain finally

$$\boxed{\psi_n = \sum_{r,s} J_r(\zeta)\, J_s(a\zeta)\, e^{-is\delta}}, \tag{28}$$

where r and s are all integers satisfying the relations

$$\boxed{n = n_1 r + n_2 s}. \tag{29}$$

Those results are in accordance with the general conclusions of the foregoing section. In the Appendix will be shown that the same solution is obtained by using the preliminary theory of Raman and Nath.

We shall now investigate the symmetry properties of the spectra of orders $-n$ and $+n$ in this special case $\rho_1 = 0$. In order to calculate the intensity of the order n from the expression for the amplitudes (28), it has proved advantageous to replace the summation indices r and s, coupled by the relation (29), by one index that goes through the row of all integers from $-\infty$ to $+\infty$. Therefore we shall put,

$$r = a + jn_2, \quad s = b - jn_1, \tag{30}$$

where $|\, a \,|$ and $|\, b \,|$ are the smallest pair of whole numbers satisfying the relation $n = n_1 a + n_2 b$; j is an arbitrary integer; the so chosen values of r and s fulfil the condition (29). The intensity $I_n = \psi_n \psi_n^*$ now reads

$$\begin{aligned} I_n &= \sum_{j=-\infty}^{\infty} J_{a+jn_2}(\zeta)\, J_{b-jn_1}(a\zeta)\, e^{-i(b-jn_1)\delta} \\ &\quad \times \sum_{k=-\infty}^{\infty} J_{a+kn_2}(\zeta)\, J_{b-kn_1}(a\zeta)\, e^{i(b-kn_1)\delta} \\ &= \sum_{j} J^2_{a+jn_2}(\zeta)\, J^2_{b-jn_1}(a\zeta) \\ &\quad + 2 \sum_{j<k} J_{a+jn_2}(\zeta)\, J_{a+kn_2}(\zeta)\, J_{b-jn_1}(a\zeta)\, J_{b-kn_1}(a\zeta) \cos(j-k) n_1 \delta. \end{aligned} \tag{31}$$

On the other hand we have

$$\begin{aligned} I_{-n} &= \sum_{j=-\infty}^{\infty} J_{-a-jn_2}(\zeta)\, J_{-b+jn_1}(a\zeta)\, e^{i(b-jn_1)\delta} \\ &\quad \times \sum_{k=-\infty}^{\infty} J_{-a-kn_2}(\zeta)\, J_{-b+kn_1}(a\zeta)\, e^{-i(b-kn_1)\delta}, \end{aligned}$$

which becomes after some calculations, where the well-known relation between Bessel functions, $J_{-n}(z) = (-1)^n J_n(z)$, has been employed

$$I_{-n} = \sum_j J^2_{a+jn_2}(\zeta)\, J^2_{b-jn_1}(a\zeta) + 2 \sum_{j<k} (-1)^{(k+j)(n_2-n_1)} J_{a+jn_2}(\zeta)\, J_{a+kn_2}(\zeta) \times J_{b-jn_1}(a\zeta)\, J_{b-kn_1}(a\zeta) \cos(j-k)\, n_1\delta. \tag{32}$$

Comparison of the expressions (31) and (32) leads to the following conclusion:

In the case $\rho_1 = 0$, *the intensities of the orders* $-$ n *and* $+$ n *are equal if* $n_1 - n_2$ *is even; those intensities are not equal if* $n_1 - n_2$ *is odd, except in the case that* n_1 *is odd and* δ *an odd multiple of* $\pi/2$.*

4. Symmetry and Asymmetry in the General Case $\rho_1 \neq 0$

If the intensities of the orders n and $-n$ should be equal, *i.e.*, $I_n = I_{-n}$ we should have either $\psi_n = e^{i\gamma_n(\zeta)}\psi_{-n}$ or $\psi_n = e^{i\gamma_n(\zeta)}\psi_{-n}^*$, where $\gamma_n(\zeta)$ is a yet arbitrary function of ζ and where ψ_{-n}^* designates the complex conjugate of ψ_{-n}.

(1) *First Possibility:*

$$\psi_n = e^{i\gamma_n(\zeta)}\psi_{-n}. \tag{33}$$

Making this substitution into the general equation (20), we obtain

$$2\frac{d\psi_{-n}}{d\zeta} - \{\psi_{-n+n_1} \exp i(\gamma_{n-n_1} - \gamma_n) - \psi_{-n-n_1} \exp i(\gamma_{n+n_1} - \gamma_n)\} - a\{\psi_{-n+n_2} \exp i(\gamma_{n-n_2} - \gamma_n)\, e^{-i\delta} - \psi_{-n-n_2} \exp i(\gamma_{n+n_2} - \gamma_n)\, e^{i\delta}\} = i\left(\rho_1 n^2 - 2\frac{d\gamma_n}{d\zeta}\right)\psi_{-n}. \tag{34}$$

If we now change n into $-n$ in equation (20), we have

$$2\frac{d\psi_{-n}}{d\zeta} - (\psi_{-n-n_1} - \psi_{-n+n_1}) - a\{\psi_{-n-n_2}\, e^{-i\delta} - \psi_{-n+n_2}\, e^{i\delta}\} = i\rho_1 n^2 \psi_{-n}, \tag{35}$$

equation that must be identical with (34).

(*a*) Identification of the second members of both equations gives $d\gamma_n/d\zeta = 0$, from which it follows that

$$\gamma_n(\zeta) = \text{constant}. \tag{36}$$

* This result has been partly derived by Mr. O. Leroy.

(*b*) Identifying the terms between the first brackets of the left-hand sides of equations (34) and (35) gives $\exp i(\gamma_{n-n_1}-\gamma_n) = -1$ and $\exp i(\gamma_{n+n_1}-\gamma_n) = -1$ from which

$$\gamma_{n-n_1} - \gamma_n = (2k+1)\pi \tag{37 a}$$

and

$$\gamma_{n+n_1} - \gamma_n = (2l+1)\pi. \tag{37 b}$$

A solution of this system of difference equations is

$$\gamma_{jn_1} = \gamma_{jn_1+1} = \gamma_{jn_1+2} = \cdots = \gamma_{jn_1+i} = \cdots = \gamma_{jn_1+n_1-1} = j\pi \qquad 0 \leqslant i \leqslant n_1 - 1. \tag{38}$$

This may easily be verified by direct substitution; we also remark that (38) gives $\gamma_0 = 0$, which is required by the form of the substitution (33). We further obtain for $n_1 = 1$, $\gamma_n = n\pi$, which is in accordance with the results of our earlier paper, treating this special case [*cf.* Ref. 6, Eq. (20)].

(*c*) The identity of the second brackets of the left-hand sides of equations (34) and (35) leads to

$$\exp i(\gamma_{n-n_2} - \gamma_n)\, e^{-i\delta} = -e^{i\delta}, \tag{39 a}$$

$$\exp i(\gamma_{n+n_2} - \gamma_n)\, e^{i\delta} = -e^{-i\delta}. \tag{39 b}$$

In order to transform those conditions, we shall now calculate $\gamma_{n-n_2} - \gamma_n$ and $\gamma_{n+n_2} - \gamma_n$.

Firstly it may always be supposed, that $n_1 < n_2\,(n_1 > 1)$. We shall further put

$$n_2 = pn_1 + q, \quad p \geqslant 1, \quad 1 \leqslant q \leqslant n_1 - 1 \tag{40 a}$$

$$n = mn_1 + i, \quad m \geqslant 0, \quad 0 \leqslant i \leqslant n_1 - 1 \tag{40 b}$$

(p, q, m and i being integers), so that

$$\gamma_{n-n_2} - \gamma_n = \gamma_{(m-p)n_1+i-q} - \gamma_{mn_1+i}, \quad -(n_1-1) \leqslant i-q \leqslant n_1-2 \tag{41 a}$$

$$\gamma_{n+n_2} - \gamma_n = \gamma_{(m+p)n_1+i+q} - \gamma_{mn_1+i}, \quad 1 \leqslant i+q \leqslant 2n_1-2 \tag{41 b}$$

from which, using (38),

$$\gamma_{n-n_2} - \gamma_n = -p\pi \quad \text{if} \quad 0 \leqslant i-q \leqslant n_1-2 \tag{42 a}$$

$$\gamma_{n-n_2} - \gamma_n = -(p+1)\pi \quad \text{if} \quad -(n_1-1) \leqslant i-q < 0 \tag{42 b}$$

$$\gamma_{n+n_2} - \gamma_n = p\pi \quad \text{if} \quad 1 \leqslant i+q \leqslant n_1-1 \tag{42 c}$$

$$\gamma_{n+n_2} - \gamma_n = (p+1)\pi \quad \text{if} \quad n_1 \leqslant i+q \leqslant 2n_1-2 \tag{42 d}$$

The combination of those possibilities leads to the following four cases:

(α) $\gamma_{n-n_2} - \gamma_n = -p\pi$ and $\gamma_{n+n_2} - \gamma_n = p\pi$ with $1 \leqslant q \leqslant n_1/2 - \frac{1}{2}$.

If p is even, the conditions (39) are equivalent with $\cos\delta = 0$, *i.e.*, $\delta = (k + \frac{1}{2})\pi$.

If p is odd those conditions may be replaced by $\sin\delta = 0$, *i.e.*, $\delta = k\pi$.

(β) $\gamma_{n-n_1} - \gamma_n = -(p+1)\pi$ and $\gamma_{n+n_1} - \gamma_n = (p+1)\pi$ with $n_1/2 < q \leqslant n_1 - 1$.

The conditions (39) may then be replaced by the following ones:

If p is even, $\sin\delta = 0$ or $\delta = k\pi$.

If p is odd, $\cos\delta = 0$ or $\delta = (k + \frac{1}{2})\pi$.

(γ) $\gamma_{n-n_1} - \gamma_n = -p\pi$ and $\gamma_{n+n_1} - \gamma_n = (p+1)\pi$.

(39 *a*) and (39 *b*) lead to the simultaneous conditions $\cos\delta = 0$, $\sin\delta = 0$ for all values of p, which are impossible to fulfil.

(δ) $\gamma_{n-n_1} - \gamma_n = -(p+1)\pi$ and $\gamma_{n+n_1} - \gamma_n = p\pi$.

Here the same impossible conditions as in the foregoing case are obtained.

(2) *Second possibility:*

$$\psi_n = e^{i\gamma_n(\zeta)}\,\psi^*_{-n}. \tag{43}$$

Substitution of this expression for ψ_n into the system (20) gives

$$\begin{aligned} 2\frac{d\psi^*_{-n}}{d\zeta} &- \{\psi^*_{-n+n_1}\exp i(\gamma_{n-n_1} - \gamma_n) - \psi^*_{-n-n_1}\exp i(\gamma_{n+n_1} - \gamma_n)\} \\ &- \alpha\{\psi^*_{-n+n_1}\exp i(\gamma_{n-n_1} - \gamma_n)\,e^{-i\delta} - \psi^*_{-n-n_1}\exp i(\gamma_{n+n_1} - \gamma_n)\,e^{i\delta}\} \\ &= i\left(\rho_1 n^2 - 2\frac{d\gamma_n}{d\zeta}\right)\psi^*_{-n}. \end{aligned} \tag{44}$$

On the other hand the complex conjugate of equation (20) in which n has been changed into $-n$ reads

$$\begin{aligned} 2\frac{d\psi^*_{-n}}{d\zeta} &- (\psi^*_{-n-n_1} - \psi^*_{-n+n_1}) - \alpha\{\psi^*_{-n-n_1}\,e^{i\delta} - \psi^*_{-n+n_1}\,e^{-i\delta}\} \\ &= -i\rho_1 n^2\psi^*_{-n}. \end{aligned} \tag{45}$$

Both equations (44) and (45) must be identic. Equating the right-hand sides gives $d\gamma_n/d\zeta = \rho_1 n^2$, which has the solution $\gamma_n = \rho_1 n^2\zeta + C_n$, C_n being a constant. Introducing this value into the first bracket of the left-hand side of equation (44) and comparing with the first bracket of (45) it is easily seen that their identity could never be realized.

Hence, we may conclude in the general case $\rho_1 \neq 0$, that in the diffraction pattern we shall have $I_n \neq I_{-n}$ as soon as one of the following conditions is fulfilled:

$$\left.\begin{array}{l} p \text{ even, } \delta \neq (k+\frac{1}{2})\pi \\ \text{or} \\ p \text{ odd, } \delta \neq k\pi \end{array}\right\} \quad \text{when} \quad 1 \leqslant q \leqslant \frac{n_1}{2} - \frac{1}{2}$$

$$\left.\begin{array}{l} p \text{ even, } \delta \neq k\pi \\ \text{or} \\ p \text{ odd, } \delta \neq (k+\frac{1}{2})\pi \end{array}\right\} \quad \text{when} \quad \frac{n_1}{2} < q \leqslant n_1 - 1.$$

The proof may easily be given by a reasoning *ab absurdo*.

So, for example, we shall have an asymmetric pattern with respect to the zero order for $n_1 = 2$ and $n_2 = 3$ ($p = q = 1$) when $\delta \neq (k + \frac{1}{2})\pi$, which corresponds with the results of the elementary theory [$n_2 - n_1$ odd, $\delta \neq (k + \frac{1}{2})\pi$]; for $n_1 = 3$, $n_2 = 5$ ($p = 1$, $q = 2$) an asymmetric pattern is to be expected when $\delta \neq (k + \frac{1}{2})\pi$, whereas the elementary theory predicts a symmetric pattern with respect to the zero order ($n_2 - n_1$ even).

We are glad to express our sincere thanks to Professor Dr. M. Nuyens for his stimulating interest in our work. Our thanks are also due to Mr. O. Leroy for some valuable suggestions.

Summary

Starting from the wave equation for the electric field of the light, the theory of the diffraction of light by two superposed supersonic waves is developed for sound waves, the frequency ratio of which is $n_1 : n_2$, where n_1 and n_2 are simple incommensurable whole numbers, different from one. A system of difference-differential equations is derived, using the Fourier series method of Raman and Nath. The diffracted light waves make angles defined by

$$\sin \theta_{rs} = -\left(\frac{r}{\lambda_1^*} + \frac{s}{\lambda_2^*}\right)\lambda$$

with the direction of the incident light and have frequency changes $-(rv_1^* + sv_2^*)$, (r, s) being all the couples of integers satisfying the relation $n = rn_1 + sn_2$, where n is the number of the diffraction order. Neglecting the right-hand side of the difference-differential equation, approximation which corresponds with very intense ultrasonic waves having great wavelengths, the exact solution of the problem is obtained by using a complex

integral method. In this special case the diffraction pattern is symmetric with respect to the zero order if $n_2 - n_1$ is even; for $n_2 - n_1$ odd, the pattern is asymmetric, except when n_1 is odd and the phase angle of the sound waves $\delta = (k + \frac{1}{2})\pi$. It has further been shown, that in the general case the intensity of the orders n and $-n$ are always different, excepting for some special values of the phase angles of the supersonic waves.

REFERENCES

1. Ramachandra Rao, M. A. *Proc. Ind. Acad. Sci.*, 1949, **29 A**, 16.
2. Murty, J. S. .. *J. Acoust. Soc. Am.*, 1954, **26**, 970.
3. Raman, C. V. and Nagendra Nath, N. S. *Proc. Ind. Acad. Sci.*, 1935, **2 A**, 406.
4. ———— .. *Ibid.*, 1936, **3 A**, 119.
5. Zankr[1], K. L. and Hiedemann, E. A. *J. Acoust. Soc. Am.*, 1959, **31**, 44.
6. Mertens, R. .. *Proc. Ind. Acad. Sci.*, 1958, **48 A**, 288.
7. Bergmann, L. and Fues, E. *Z. Physik.*, 1938, **109**, 1.
8. Nagendra Nath, N. S. .. *Proc. Cambr. Phil. Soc.*, 1938, **34**, 213.
9. Nagabhushana Rao, K. .. *Proc. Ind. Acad. Sci.*, 1938, **8 A**, 124.
10. Bergmann, L. .. *Z. Hochfrequenztech.*, 1934, **43**, 83.
11. Watson, G. N. .. *Treatise on the Theory of Bessel Functions*, Cambridge, 1944, p. 14.
12. ———— .. *Ibid.*, p. 22.

APPENDIX

Derivation of the Results of § 3 by the Method of Raman and Nath's Elementary Theory[3]

Let L be the width of the sound field, then the outgoing light wave in the plane $z = L$ can be written as

$$\phi(x, L, t) = \exp 2\pi i\nu \left\{t - \frac{L}{c}\mu(x, t)\right\}$$

$$= \exp 2\pi i\nu t \cdot \exp - \frac{2\pi i L\mu(x, t)}{\lambda}, \qquad \text{(A.1)}$$

where c is the velocity of the light in vacuum, or using the explicit expression (3) for the refractive index

$$\phi(x, L, t) = \exp 2\pi i\nu t \cdot \exp - 2\pi i \frac{\mu_0 L}{\lambda}$$

$$\times \exp\left\{- 2\pi i\mu_1 \frac{L}{\lambda} \sin 2\pi\left(\nu_1^* t - \frac{x}{\lambda_1^*}\right)\right\}$$

$$\times \exp\left\{- 2\pi i\mu_2 \frac{L}{\lambda} \sin 2\pi\left(\nu_2^* t - \frac{x}{\lambda_2^*} + \Delta\right)\right\}. \qquad \text{(A.2)}$$

Developing the last two exponentials in a series of Bessel functions[12] we obtain

$$\phi(x, L, t) = \exp 2\pi i\nu t \cdot \exp - 2\pi i \frac{\mu_0 L}{\lambda}$$

$$\times \sum_{r=-\infty}^{\infty} (-1)^r \exp 2\pi i\left(r\nu_1^* t - \frac{r}{\lambda_1^*} x\right) J_r\left(\frac{2\pi L\mu_1}{\lambda}\right)$$

$$\times \sum_{s=-\infty}^{\infty} (-1)^s \exp 2\pi i\left(s\nu_2^* t - \frac{s}{\lambda_2^*} x + s\Delta\right)$$

$$\times J_s\left(\frac{2\pi L\mu_2}{\lambda}\right).$$

Changing r into $-r$, s into $-s$ and taking into account the relation $J_{-n}(z) = (-1)^n J_n(z)$ it follows that

$$\phi(x, L, t) = \exp 2\pi i\nu t \cdot \exp -\frac{2\pi i\mu_0 L}{\lambda}$$

$$\times \sum_{r,s=-\infty}^{\infty} J_r\left(\frac{2\pi\mu_1 L}{\lambda}\right) J_s\left(\frac{2\pi\mu_2 L}{\lambda}\right) e^{-is\delta}$$

$$\times \exp -2\pi i\,(r\nu_1^* + s\nu_2^*)\,t$$

$$\times \exp 2\pi i\left(\frac{r}{\lambda_1^*} + \frac{s}{\lambda_2^*}\right) x. \qquad \text{(A.3)}$$

This is the formula already obtained by Nagendra Nath[8] for two completely arbitrary supersonic waves. From this formula it is seen, that the light wave diffracted in the direction

$$\sin\theta_{rs} = -\left(\frac{r}{\lambda_1^*} + \frac{s}{\lambda_2^*}\right)\lambda$$

undergoes a frequency change

$$\Delta\nu_{rs} = -(r\nu_1^* + s\nu_2^*)$$

and has the amplitude

$$\phi_{rs} = J_r(\nu_1)\, J_s(\nu_2)\, e^{-is\delta},$$

where

$$\nu_i = \frac{2\pi\mu_i L}{\lambda} \qquad (i = 1, 2).$$

Introducing now for our case the relations (4) and (5) and grouping together all terms in the series (A.3) for which r and s satisfy the relation $n = n_1 r + n_2 s$, we may conclude that the whole spectrum is composed of waves in the direction θ_n defined by $\sin\theta_n = -n\lambda/\Lambda$, having a frequency change $-nN$ and having a total amplitude

$$\psi_n = \sum_{n_1 r + n_2 s = n} \phi_{rs} = \sum_{n_1 r + n_2 s = n} J_r(\nu_1)\, J_s(\nu_2)\, e^{-is\delta} \qquad \text{(A.4)}$$

which is nothing else but the amplitude (28) for $z = L$.

SUM-COINCIDENCE TECHNIQUE FOR γ-RAY STUDIES

By S. Jha, H. G. Devare, M. Narayana Rao and Kumari G. C. Pramila

(Tata Institute of Fundamental Research, Bombay)

Received July 18, 1959

(Communicated by Dr. B. V. Thosar, F.A.SC.)

Introduction

Hoogenboom (1958) has recently developed, for the study of γ-rays in cascade, a new technique in scintillation spectrometry which he calls the "sum-coincidence" method. He applied this method to the study of the γ-rays emitted in the decay of Co^{60} and Na^{22} and of the γ-rays emitted in the (p, γ) reactions. In this paper the results of the application of this method to the decay of Sc^{46}, Sm^{153} and Eu^{154} are reported. It has been found that this method helps in detecting low intensity γ-rays emitted in cascade and it is a powerful tool in the estimation of the relative intensities of the alternative cascade emission of γ-rays. For the decay of Eu^{154}, this method has been used in identifying a level at 1850 Kev. as belonging to Gd^{154}.

Description of the Method

If a radioactive source emitting γ-rays in cascade is viewed by two well-matched NaI (Tl) crystals and photomultiplier units, and the pulse outputs from the two units are added up electronically and analysed in a pulse height analyser, the spectrum will show, in addition to the Compton humps and the individual photo-peaks, the sum peak of the γ-rays in cascade. For instance, in Sc^{43}, in addition to the Compton humps and the photo-peaks of the 880 Kev. and the 1120 Kev. γ-rays, one would observe a peak at 2004 Kev. Now, if one takes this sum peak in the gate of the coincidence unit and scans the spectrum in one of the units, one would observe the photo-peaks of only those γ-rays which are members of the cascade and whose energies add up to the sum peak energy. The Compton pulses not contributing to the sum peak would be suppressed completely. Secondly, if only a narrow band of the sum peak is taken in the gate, the photo-peaks in the sum-coincidence spectrum of the cascade γ-rays look very much sharper.

In the experiments being reported here, two NaI crystals $1\frac{1}{2}''$ in diameter, $2''$ thick attached to two DuMont 6292 photomultipliers, were used. The cathode-follower output of one of the units was divided into two, one being connected through an adder circuit to the cathode-follower of the second unit, and the added output fed to a linear amplifier and a pulse height analyser; the other was connected directly to an amplifier and a pulse height analyser. These two branches were fed into a slow-fast coincidence unit, a small portion of the sum peak from the added spectrum served as the gate, and the cathode-follower output was analysed in coincidence. Figure 1 gives the electronic arrangement.

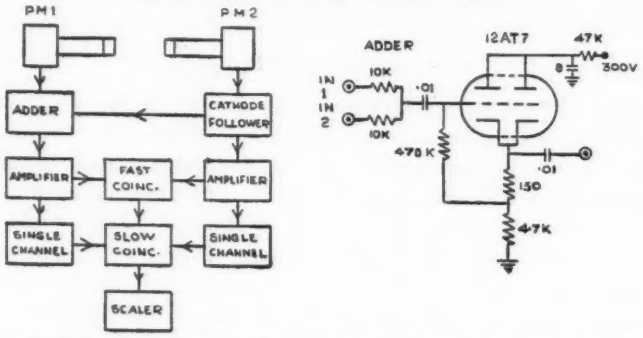

FIG. 1.—(*a*) The block diagram of the electronic equipments for the "sum-coincidence" studies.

(*b*) Adder circuit.

EXPERIMENTAL RESULTS

In this section, the results of our study of a number of isotopes by the "sum-coincidence" technique are described.

Sum-Coincidence Study of Sc^{46}

Sc^{46} decays almost entirely by the emission of 357 Kev. β-rays to the second excited state of Ti^{46} at 2·004 Mev., followed by the emission of 885 Kev. and 1120 Kev. γ-rays. When the source was sandwiched between two well-matched NaI crystals, and multiplier units one got a sum peak of the two γ-rays at 2·004 Mev. A part of this sum peak (about 2 volts) was taken in the gate and the spectrum in coincidence was scanned. Figure 2 (*a*) gives the ordinary spectrum of Sc^{46}. Figure 2 (*b*) gives the spectrum in coincidence with the sum peak. One can see that the Compton hump has disappeared completely. The last peak at 2·004 Mev. is due to the adding of the two γ-rays in the scanning crystal. The half-width of the 1·12 Mev. γ-ray is about 5%.

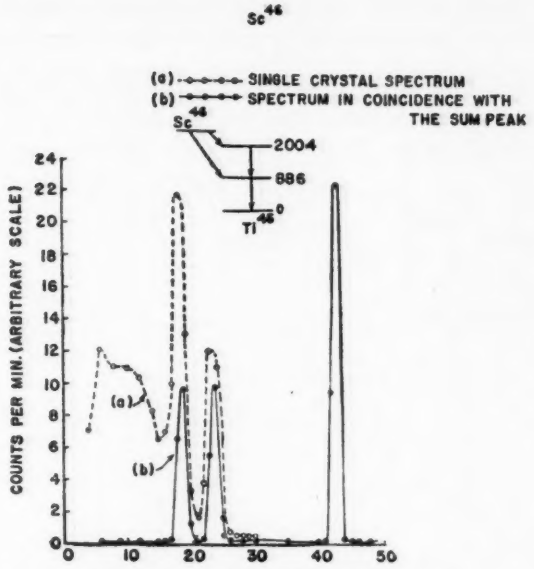

FIG. 2. (*a*) Single spectrum of Sc^{46} γ-rays.
(*b*) "Sum-coincidence" spectrum of the γ-rays of Sc^{46}.

Sum-Coincidence Study of Sm^{153}

The next isotope studied by this technique was the 47 hr. Sm^{153}. This isotope decays by β-emission mainly to the ground state and to the states at 103 Kev. and 170 Kev. of Eu^{153}. The γ-rays associated in the decay of this isotope are the cascade γ-rays of energy 70 Kev. and 103 Kev. and the cross-over γ-ray of energy 170 Kev. Due to the internal conversion of γ-rays, 40 Kev. K X-ray of $_{63}Eu$ is also emitted. The decay scheme is shown in Fig. 3 *a*.

When the source of Sm^{153} is placed in between two NaI crystals for "the sum-coincidence studies", the added spectrum shows (Fig. 3 *b*) the K X-ray, 70 Kev. γ-ray, 103 Kev. γ-ray, a peak at 144 Kev. due to the summing of the 103 Kev. γ-ray and the K X-ray of Eu arising from the internal conversion of the 70 Kev. γ-ray, and finally an enhanced peak at 170 Kev. due to the 170 Kev. γ-ray and due to the summing of the 103 Kev. γ-ray and the 70 Kev. γ-ray. Now, if one takes a small portion of the sum peak at 143 Kev. in the gate and scans the spectrum in one of the crystals, one should get the sum-coincidence peaks only at 40 Kev., 103 Kev. and at 143 Kev. The peak at 70 Kev. should be completely suppressed because the 70 Kev. γ-ray

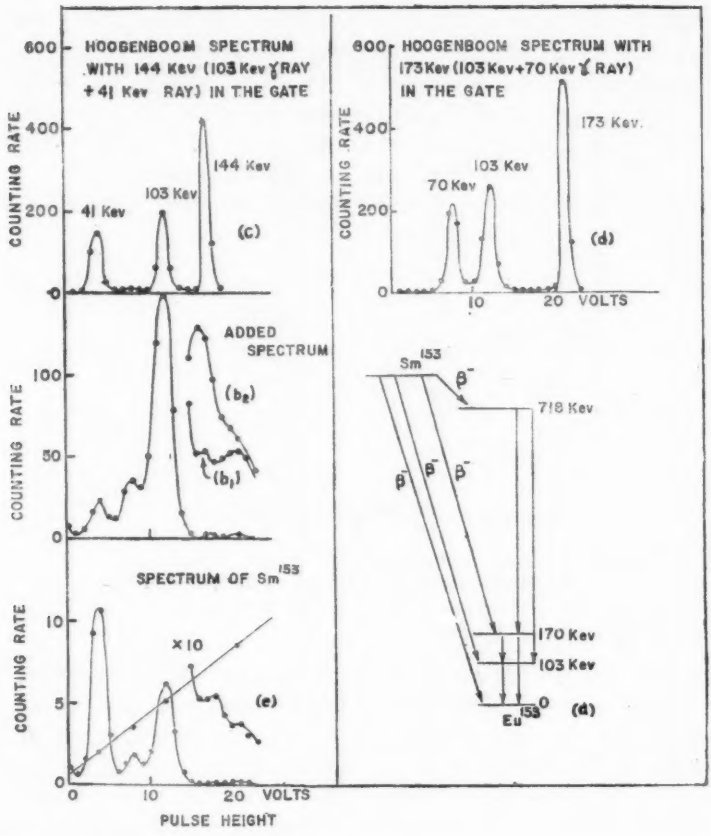

FIG. 3. (*a*) Decay scheme of Sm^{153}.

(*b*) Added spectrum of the γ-rays of Sm^{153}.

(b_1) The K X-rays have been absorbed to bring into prominence the peak at 170 Kev.

(b_2) K X-rays have not been absorbed and one gets a strong peak at 144 Kev. (103 Kev. + 41 Kev.).

(*c*) "Sum-coincidence" spectrum with 144 Kev. sum peak in the gate.

(*d*) "Sum-coincidence" spectrum with 173 Kev. sum peak in the gate.

does not contribute to the peak at 143 Kev. This is what one finds as shown in Fig. 3 *c*. On the other hand, if one selects a small portion of the sum peak at 173 Kev. and scans the spectrum in one of the crystals, one should get the sum-coincidence peaks at 70 Kev., 103 Kev. and at 173 Kev. The 40 Kev.

K X-ray peak should be suppressed completely. This is shown in Fig. 3 *d*.

Eu^{154}

The sum-coincidence technique has been used to study the complicated decay scheme of Eu^{154}. The decay scheme of this isotope has been given by Juliano and Stephens (1957), Cork *et al.* (1957) and by Bhattacharji *et al.* (1958). It is reproduced in Fig. 4.

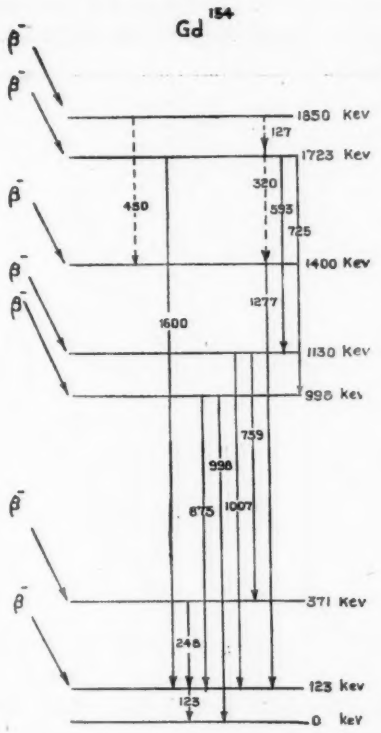

FIG. 4. The decay scheme of the Eu^{154}, including a level at 1850 Kev. in Gd^{154}.

The highest energy level in Gd^{154}, known so far, is the level at 1723 Kev. which decays with the emission of the following cascades: (*a*) 725 Kev. + 998 Kev., (*b*) 725 Kev. + 875 Kev. + 123 Kev., (*c*) 593 Kev. + 1007 Kev. + 123 Kev., (*d*) 593 Kev. + 760 Kev. + 244 Kev. + 123 Kev., and (*e*) 1600 Kev. + 123 Kev. If one puts the 1723 Kev. sum peak in the gate and observes the "sum-coincidence" spectrum, one should get only these γ-rays. For instance, one should not observe the 1277 Kev. γ-ray if there

is no transition from the 1723 Kev. state to the 1400 Kev. state with the emission of 323 Kev. γ-ray.

For the present studies, a weak source of Eu^{154}, made from the neutron irradiation of enriched Eu^{153} in the reactor at Oak Ridge, was used. As described earlier, the source was viewed by two well-matched NaI crystals and multiplier units, and the pulses were added with a resistance network. The spectrum of γ-rays in a single unit is given in Fig. 5. The added spectrum of γ-rays is given in Fig. 6. In the added spectrum, one finds a peak occurring at 1723 Kev. corresponding to the highest known level at 1723.

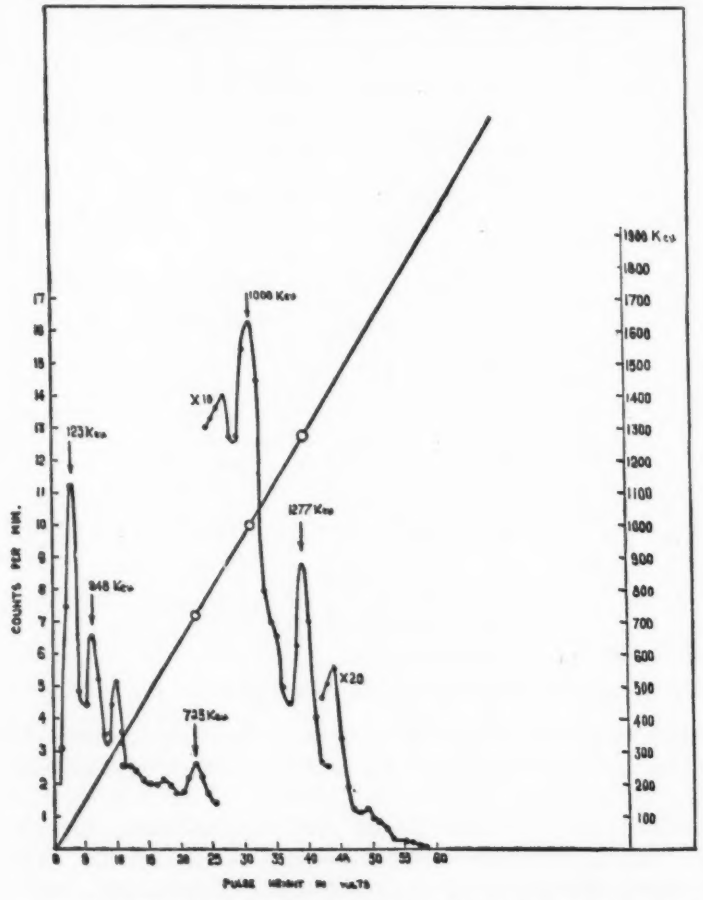

FIG. 5. γ-Spectrum of Eu^{154} with the source in contact with the crystal.

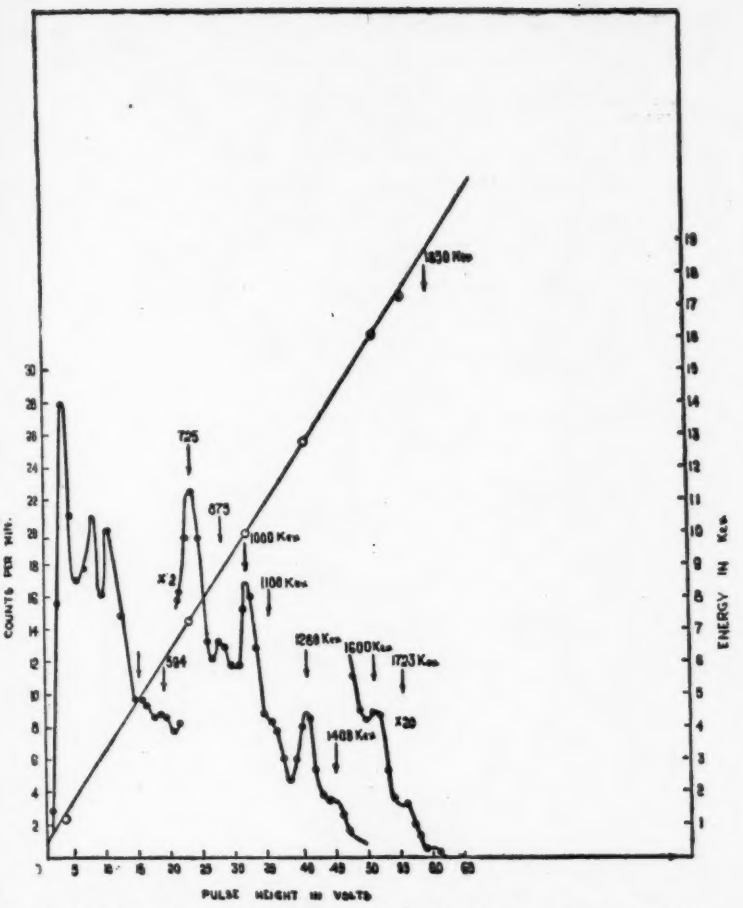

FIG. 6. Added spectrum of the γ-rays of Eu^{154} showing sum peaks at 1723 Kev. and 1850 Kev.

In addition, one can see that there is a peak at 1,850 Kev. also. The latter peak may be due to a hitherto unreported level in Gd^{154} or it may due to some impurities. By studying the height of this peak with different intensity sources, it was concluded that this peak did not arise from the random summing of γ-rays.

First a small portion (one volt) of the sum peak at 1723 was taken in the gate and the spectrum in one of the crystals was scanned in a twenty-channel pulse-height analyser. The sum-coincidence spectrum is reproduced

in Fig. 7. Here one can see the peaks at the γ-ray energies 123 Kev., 248 Kev., 330 Kev., 725 Kev., 875 Kev., 1000 Kev., 1277 Kev., 1400 Kev., 1600 Kev.

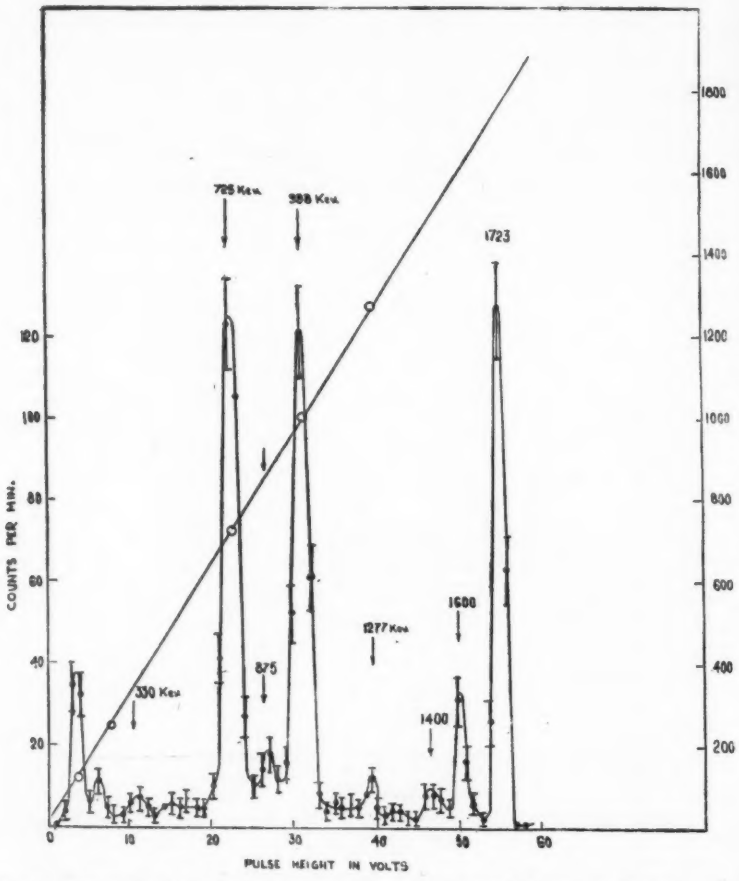

FIG. 7. "Sum-coincidence" spectrum of the γ-rays of Eu^{154} with 1723 Kev. sum peak in the gate.

and at 1723 Kev. Of the predicted γ-ray peaks, only that of 593 Kev. does not seem to have been formed properly. On the other hand, the appearance of the peaks in the sum-coincidence spectrum at 320 Kev. and 1280 Kev. points to the conclusion that some transition from 1723 Kev. level takes place to the 1400 Kev. level also.

From the unexpected appearance of a sum peak at 1850 Kev., one can only conclude (Lu *et al.*, 1954, 1955) that there is a level either in Gd^{154} or in some impurities present at this energy. The sum-coincidence techniques can be utilized to identify the source of this level. If this sum peak arises from some impurities, the γ-rays appearing in the sum-coincidence spectrum would be very different from the familiar γ-rays in the decay of Eu^{154}. Figure 8 shows the "sum-coincidence" spectrum with the 1850 Kev. sum peak

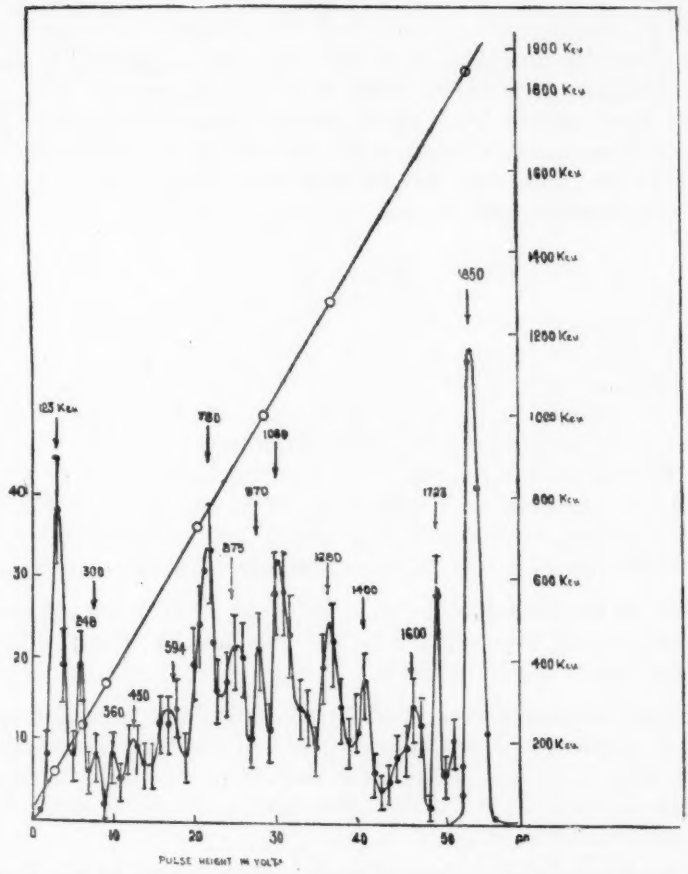

FIG. 8.—"Sum-coincidence" spectrum of the γ-rays of Eu^{154} with 1850 Kev. sum peak in the gate.

(2 volts) in the gate. The γ-ray peaks appear at about 123 Kev., 248 Kev., 300 Kev., 360 Kev., 450 Kev., 594 Kev., 760 Kev., 875 Kev., 970 Kev.,

1060 Kev., 1280 Kev., 1400 Kev., 1600 Kev., 1723 Kev., and 1850 Kev. Of these, the peaks at 1723 Kev., 1600 Kev., 1400 Kev., 1280 Kev., 1000 Kev., 594 Kev., 248 Kev. and 123 Kev. are familiar in the decay of Eu^{154}. One is thus inclined to think that there is a level in Gd^{154} at 1850 Kev. which is fed to a small extent by the beta decay of Eu^{154}. From the relative magnitude of the sum peak areas at 1723 Kev. and at 1850 Kev. (Bhatki, Gupta and Jha, 1956), one can calculate the relative intensities of the β^--branchings. If the conclusion is correct, β^--branching leading to the 1850 Kev. level is about 3%.

No effort has been made to fit the other peaks appearing in the sum-coincidence spectrum of Eu^{154} with the 1850 Kev. sum peak in the gate into the Eu^{154} decay scheme. The present decay scheme is obviously not adequate as it cannot account for the peaks near 1100 Kev., the complex nature of the 1600 Kev. peak, and the 694 Kev. and 705 Kev. peaks found by Juliano and Stephens (1957).

DISCUSSION

The sum-coincidence technique is extremely powerful in revealing rare modes of decay of cascade γ-rays, as shown in the case of Eu^{154}, Tl^{202} (Jha and Devare, 1959), Ba^{133} (Jha *et al.*, 1959). If a state A decays by the emission of a dominant cascade X and Y, and a weaker cascade M and N, it is found that within the statistics, the height of the peaks X and Y are equal, and those of M and N are equal. The ratio of the peak areas (X or Y)/(M or N) is a measure of the intensity ratio of the two modes of decay. Of course, if one wants to be precise, one should include corrections for the internal conversion of γ-rays and for efficiencies of detection of the γ-rays.

It may be emphasised here that in the study of Eu^{154} the technique of sum-coincidence has been utilised for the identification of the 1850 Kev. level as the one belonging to Eu^{154}.

In course of these studies, it was realised that this technique can be utilised with profit only if one makes use of well-matched NaI crystals and multiplier units of the best quality. The stability of the high voltage supply required in this case is much greater than what is needed in ormal scintillation spectrometer studies.

Our work was greatly facilitated by the generous help of Dr. B. Saraf, who placed his twenty-channel pulse-height analyser at our disposal. We express our deep appreciation of the help we have received from M/s. R. M. Singru, Jambunathan and Deshpande.

Summary

If a radioactive source emitting cascade γ-rays is placed between two well-matched NaI crystal and multiplier units and pulses from the two units are added electronically, one would get, in the added spectrum, a peak corresponding to the sum of the energies of the cascade γ-rays. If the pulses in one of the units are analysed in coincidence with the final sum peak, one would get only the photo-peaks of the cascade γ-rays. This "sum-coincidence" technique has been applied to the study of the γ-rays of Sc^{46}, Sm^{153} and Eu^{154}. In Eu^{154} decay, the cascade emission of 320 Kev., 1280 Kev. and 123 Kev. γ-rays has been established; and it has been shown that there is a level in Gd^{154} at 1850 Kev. which is fed by β^--emission from Eu^{154} to the extent of about 3%.

References

Bhatki, K. S., Gupta, R. K. and Jha, S. — *Nuovo Cimento*, Series X, 1956, **4**, 1519.

Bhattacharji *et al.* .. *Proc. Ind. Acad. Sci.*, 1958, **47**, 295.

Cork, J. M., Brice, M. K., Helmer, R. G. and Sarason, D. E. — *Phys. Rev.*, 1951, **107**, 1621.

Hoogenboom, A. M. .. *Nuclear Instruments*, 1958, **3**, 57.

Jha, S. and Devare, H. G. .. To be published, 1959.

—— *et al.* .. To be published, 1959.

Juliano, J. O. and Stephens, F. S. — *Phys. Rev.*, 1951, **108**, 341.

Lu, D. C., *et al.* .. *Ibid.*, 1954, **94**, 501.
Ibid., 1954, **95**, 121.
Ibid., 1954, **95**, 1533.
Ibid., 1955, **97**, 139.

THE DARK COLOUR OF BLACK COTTON SOILS

By V. S. Ramachandran, F. U. Ahmad and L. C. Jain

(Central Building Research Institute, Roorkee)

Received May 30, 1959

(Communicated by Prof. T. N. Seshadri, F.A.SC.)

Introduction

The paper deals with investigations into the properties of organic matter in black cotton soils and attempts to explain the factors responsible for the dark colour of the soil. The dark colour was previously attributed to the presence of titaniferrous magnetite,[1] magnetite,[2] a high C: N ratio,[3] exchangeable calcium,[4] the clay substance itself or organic matter.[6] Organic carbon as the cause of the black colour was discredited[7–8] as it was found that the colour was unaffected by treatment with H_2O_2 or NaOH. The conclusions reached were at variance with one another, and many of the results reported were not confirmed by subsequent investigations. No systematic analysis was carried out before and after treatment and the colour changes were observed mainly by visual observations and hence subjectively.

In the present paper an objective and systematic approach is made. Colour changes are estimated by a tintometer and expressed in terms of Munsell notation.[12] The organic carbon content was estimated before and after the treatments and the DTA technique was employed to study the thermal characteristics of the reactions involved. It is hoped that the results reported here afford an acceptable solution to the problem and throw some light, not only on the agricultural use of the soil and soil genesis, but also prove helpful in brick-making and similar industries where such soils are used.

Experimental

A typical sample of black cotton soil obtained from a brick field from Indore, Madhya Pradesh, was taken for the investigations. The mechanical analysis of the soil was carried out using sodium hexametaphosphate as the dispersing agent. The soil was also chemically analysed. The base exchange capacity was found out. These results are given in Table I. Organic carbon content was estimated by the Walkley and Black method.[9]

TABLE I

Composition of black soil from Indore

(*a*) *Mechanical composition* (*soil*)

Clay (·002 mm.)	Silt (·02 mm.)	Sand
53·3	19·8	26·9

(*b*) *Chemical composition* (*clay fraction*)

	Per cent.
SiO_2	48·65
Al_2O_3	12·83
Fe_2O_3	9·35
K_2O	Traces
TiO_2	Traces
CaO	7·87
MgO	2·26
Insolubles	1·49
Loss on ignition	17·33
SiO_2/Al_2O_3	6·42
$SiO_2/Al_2O_3 + Fe_2O_3$ ..	4·39

Different treatments, such as heating in air or vacuum and treatments with different oxidising agents and soil extractants were tried. The colour changes, observed in each of these cases, using a tintometer and expressed in terms of the Lovibond scale and Munsell notation, are given in Tables II and III. The value of the neutral tint tabulated is a measure of the dullness of the colour.

Differential thermal analysis was carried out semi-automatically on the treated and untreated soil samples. The temperature of the furnace was raised uniformly at a rate of 10° C./min. using a Leeds and Northrup Programme Controller triggered by a chromel-alumel thermocouple, placed outside the specimen block. The specimen block was of Grimshaw and Roberts pattern[10] and was made of ceramic material. The differential thermocouple, made of chromel-alumel was connected to a sensitive Galvanometer. The Galvanometer readings were taken manually. The thermograms obtained are given in Fig. 1.

TABLE II

Effect of heat treatment on the removal of colour and organic matter in black cotton soil

Sample No.	Treatment	Organic carbon %	Colours on Lovibond scale			Neutral	Visual colours (Calculated from colours on Lovibond scale)						Munsell value
			Red	Yellow	Blue		Red	Yellow	Blue	Green	Violet	Orange	
1	No treatment (original soil)	0·45	3·0	4·6	3·0	3·0	..	1·6	..	..	..	..	4/2 (10 YR) Dark grey brown
2	Heated at 100° C. (4 hrs.)	0·48	3·0	4·5	3·1	3·0	..	1·4	..	0·1	..	..	do.
3	Heated at 200° C. (4 hrs.)	0·41	3·2	4·7	3·3	3·2	..	1·4	..	0·1	..	..	do.
4	Heated at 300° C. (4 hrs.)	0·16	3·8	5·3	2·7	2·7	..	1·5	..	..	..	1·1	4/4 (7·5 YR) dark brown
5	Heated at 400° C. (4 hrs.)	0·02	4·4	5·4	1·6	1·6	..	1·0	..	..	..	2·8	5/6 (7·5 YR) strong brown
6*a*	Heated at 300° C. (vacuum) 4 hrs.	..	3·7	5·3	4·5	3·7	..	0·8	..	0·8	..	..	..
6*b*	Heated at 400° C. (vacuum) 4 hrs.	0·39	4·6	6·2	6·0	4·6	..	0·2	..	1·4	..	..	3/1 (10 YR) very dark grey

TABLE III

Change in colour and organic matter of Indore black soil after various treatments

Sample No.	Treatment	Organic carbon %	Colours on Lovibond scale			Neutral	Visual colours (Calculated from colours on Lovibond scale)						Munsell value
			Red	Yellow	Blue		Red	Yellow	Blue	Green	Violet	Orange	
1	Soil treated with hexametaphosphate and heated in vacuum at 400° C. (4 hrs.)	..	4·2	5·8	5·5	4·2	..	0·3	..	1·3	..	..	..
2	Soil treated with acidified dichromate and heated in vacuum at 400° C. (4 hrs.)	..	3·8	5·0	1·8	1·8	..	1·2	..	..	..	2·0	..
3	Sodium hydroxide, 10%	0·20	3·0	4·0	2·3	2·3	..	1·0	..	..	..	0·7	..
4	Potassium dichromate acidified with sulphuric acid (6 hrs.)	..	2·7	3·3	1·8	1·8	..	0·6	..	..	..	0·9	..
5*a*	Sodium hexametaphosphate N/25	..	2·2	3·2	2·1	2·1	..	1·0	..	..	..	0·1	..
5*b*	Sodium hexametaphosphate, 10%	0·20	1·4	1·7	1·2	1·2	..	0·3	..	..	..	0·2	7/2 (10 YR) light grey
6*a*	Hydrogen peroxide (cold)	0·39	2·7	3·5	2·7	2·7	..	0·8	..	..	..	..	..
6*b*	Hydrogen peroxide at 80° C.	0·00	2·1	3·3	1·2	1·2	..	1·2	..	..	..	0·9	6/3 (10 YR) pale brown
7	10% Ammonia	0·43	3·2	4·5	3·2	3·2	..	1·3	..	..	..	..	..

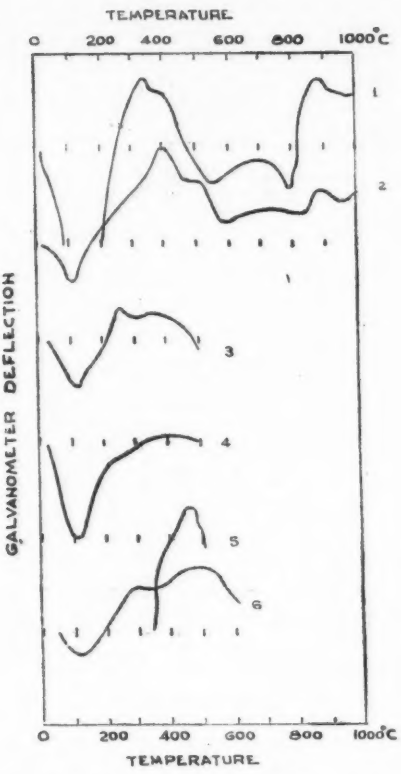

FIG. 1. Thermograms of black cotton soils subjected to various treatments.
(1) Clay fraction. (2) Vacuum-heated at 400° C. (3) Sodium hexametaphosphate treated. (4) Hydrogen peroxide (hot). (5) Hydrogen peroxide (cold). (6) Sodium hydroxide.

DISCUSSION OF RESULTS

The sample of Indore soil contains about 54% clay fraction. The base exchange capacity is 53·6 m.e./100 gm. when referred to the total soil and about 100 m.e./100 gm. when referred to the clay fraction alone. The SiO_2/Al_2O_3 and SiO_2/R_2O_3 ratios are 6·42 and 4·39 respectively and K^+ is present only in traces. These results, as well as the DTA diagrams, indicate the presence of montmorillonite in the sample.

The organic carbon content of the soil as determined is 0·45%. This is reduced to 0·16% and 0·02% when the soil is heated in air to 300° C. and 400° C. respectively with a progressive decrease, within this temperature range. The colour of the sample gradually changes as indicated by the

reduction in the neutral tint to 2·7 at 300° C. and finally to 1·6 at 400° C. The increase in red observed is to be ascribed to the sintering of Fe_2O_3. The corresponding DTA curve of the untreated soils with a strong exothermic peak at 325° C., followed by another at 410° C., should represent a stepwise oxidation of the organic content of the soil. The rest of the reactions indicated at higher temperatures represent the loss of lattice water and the breakdown of the lattice. The initial endothermic peak between 100 and 200° C. indicates loss of physically held water only.

Heating the soil to 400° C. in vacuum on the other hand increased the dark colour, the neutral tint increasing from an initial value 3·0 to 4·6 for the treated soil. The carbon content was naturally not reduced and remained at 0·39% at 400° C. The small reduction of 0·06% carbon is probably due to some burning of the organic matter to elemental carbon which cannot be detected in the Walkley and Black method. The vacuum-heated soil when heated in air loses the dark colour, above 600° C., at about which temperature the elemental carbon is oxidised. The higher endothermic peaks in the DTA curve of the vacuum-heated sample is reduced to a small extent.

Treatment with hydrogen peroxide.—Treatment with hydrogen peroxide at room temperature failed to remove the dark colour of the sample, the neutral tint reduced from 3·0–2·7 only and the organic matter from 0·45–0·39% only. This observation is in conformity with those of other workers.[6–8]

However, when the soil was treated with hydrogen peroxide at 80° C. for 6 days, the carbon content was reduced almost to 0% and the neutral tint fell from 3·0–1·2 indicating the removal of the dark colour. Worall[11] reported that lignin humus fraction of clay got oxidised by H_2O_2 treatment only at 80° C. The DTA diagram of the soil so treated fails to show the exothermic peaks whereas the diagram for the soil after cold treatment continues to show them.

Dichromate treatment.—Treatment with acidified potassium dichromate destroyed the dark colour of the sample, reducing the neutral tint from 3–1·8. When the dichromate-treated sample was heated in vacuum it failed to show any deepening of the colour. This indicates the absence of organic matter in the sample and also shows that the deepening of the dark colour in the soil on heating under vacuum is due to the reduction of the part of organic matter to elemental carbon.

Extraction with sodium hydroxide.—Using Worall's method,[12] 150 gm. of black soil was repeatedly extracted with 500 c.c. of 10% NaOH at boiling

point. The colour was only partially transferred to the alkaline extract which on addition of HCl precipitated a small amount of humic acid. The treated sample, on analysis, gave 0·3% carbon only. The neutral colour value of the residue changed from 3·0–2·3 only. Evidently NaOH could remove the colour only to a minor extent. Such would not be the case if the organic matter in the original soil contained free humic acid. This is further supported by the fact that extraction with a hot solution of ammonia did not also reduce the colour. Negative results were recorded when lignin was sought to be detected by the standard phloroglucinol and sodium hypochlorite and sodium sulphite tests. Only a small reduction of the exothermic peaks is observed for the NaOH-treated sample.

Extraction with sodium hexametaphosphate.—This method was found successful at Rothamsted[13] for extracting soil humus matter. The present sample when extracted with N/25 hexametaphosphate did not prove effective in the removal of dark colour. On the other hand, when the soil was extracted with 10% boiling solution of the hexametaphosphate, the neutral value was brought down to 1·2 and the carbon content reduced to 0·2%. The DTA diagram of the soil so treated shows the highly reduced peaks due to the residual organic matter only which is not responsible for the dark colour.

The DTA curve of the untreated sample shows that oxidation of organic matter occurs in two stages as shown by the two peaks, one at 325° C. and the other at 410° C. Soveri[14] observed double exothermic peaks in certain Fennoscandian clays. He has shown that the peak at 330° C. is caused by water-soluble or precipitated humic complexes. In some cases he observed another less pronounced peak at about 380–470° C. Thermograms of the sample treated with cold hydrogen peroxide exhibits a single exothermic peak corresponding to a temperature of 410° C. The treatment does not reduce the dark colour of the soil. Hot hydrogen peroxide practically eliminates both the peaks and also removes the dark colour. This indicates that the fraction of organic matter responsible for the dark colour is oxidised at 410° C. Phosphate treatment reduces the intensity of the dark colour as well as the area of the two peaks appreciably. Removal of humic acid from soil by phosphate treatment shows that a part of the organic matter forms a complex with the clay mineral. Sodium hydroxide treatment also reduces the area of both the peaks, but the reduction in area is much less than that obtained by the phosphate treatment. This corroborates the fact that phosphate ions are more efficacious in removing the anions which are attached on the positive sites available on the edges of the clay crystal. All this evidence points to the fact that part of the organic matter in black soil forms

a complex with the clay mineral and part is in the uncombined state. The existence of clay complex has now been well established. The fraction which combines with clay mineral is naturally more resistant to the action of the destructive agencies and therefore requires prolonged H_2O_2 treatment at a temperature of 80° C. for its destruction. It also oxidises at a higher temperature compared to other fraction.

Thus, the presence of 0·45% organic carbon in the sample, the fact that a sensible reduction of that percentage by either methods adopted is always accompanied by the destruction of dark colour and the fact that whenever there is no reduction of carbon content, the dark colour continues to persist, shows that the colour of the black soil is primarily due to its organic content, which may, in part at least, be in combination with the clay mineral.

Summary

Black cotton soil from Indore (Madhya Pradesh) which is predominantly composed of montmorillonite contained 0·45% organic matter. A sensible reduction of the organic content by any method was invariably followed by a corresponding reduction in its dark colour. Treatment with 10% sodium hexametaphosphate at boiling point or with H_2O_2 at 80° C. or the dichromate were effective in removing the colour. NaOH does not remove the organic matter nor the dark colour of the soil except only slightly. Heating in air at 400° C. oxidises the organic matter and hence removes the colour. Heating in vacuum however is obviously ineffective. DTA studies show that the oxidation of the organic matter, which is responsible for the dark colour, occurs in stages at 325° and 410°C.

Acknowledgements

The authors wish to thank the Director, Central Building Research Institute, Roorkee, for permission to publish this paper and Dr. N. K. Patwardhan for useful suggestions in compiling it. The authors are also grateful to the staff of the Central Fuel Research Institute, Dhanbad, for carrying out carbon estimations at our request.

References

1. Annet, H. E. .. *Mem. Dept. Agr., India*, 1910, No. 9, 185.
2. Del Villar, E. H. .. *Soil Sci.*, 1944, **57**, 313.
3. Mukherji, B. K. and Das, N. K. *Ind. Jour. Agric. Sci.*, 1942, **12**, 313.
4. Ashgar, A. G., Dhawan, C. L. and Bhola, K. D. *Ibid.*, 1949, **19**, 21.

5. Milne, G. *et al.* .. *Arrami Memoirs*, 1936, **34.**

6. Anon .. *Central Water and Power Research Station, Poona, Annual Report*, 1956, 115.

7. Ray Chaudhuri, S. P. .. "Symposium on black and red soils of S. India," *Indian Soil Sci.*, 1939, p. 2.

8. ——, Sulaiman, M. and Bhuiyan, A. B. *Ind. Jour. Agric. Sci.*, 1943, **13,** 264.

9. Piper, C. S. .. *Soil and Plant Analysis*, University of Adelaide, Adelaide, 1947, p. 223.

10. Grimshaw, R. W., Heaton, E. and Roberts, A. L. *Trans. Brit. Cer. Soc.*, 1945, **44,** 69.

11. Worall, W. E. and Green, C. V. *Ibid.*, 1953, **52,** 528.

12. ——— .. *Ibid.*, 1956, **55,** 689.

13. Bear, F. E. .. *Chemistry of the Soil*, Reinhold Publishing Corporation, N.Y., 1955, p. 160.

14. Soveri, U. .. *Annales Acad. Scientiarum Fennicæ*, Series A, III, 1950.

THE ABSORPTION AND FLUORESCENCE SPECTRA OF URANYL NITRATE SOLUTIONS AT ROOM TEMPERATURE

By D. D. Pant and D. P. Khandelwal

(Department of Physics, D.S.B. Government College, Nainital)

Received April 6, 1959

(Communicated by Prof. R. K. Asundi, F.A.SC.)

1. Introduction and Experimental Procedure

Nichols and Coworkers (1914–19) described the fluorescence spectra of solutions of uranyl nitrate and observed a variety of changes in the frozen state spectra. The approximate coincidence of room temperature spectrum of the solution with that of the solid led Levshin (1937) to suggest that undissociated molecules were responsible for the fluorescence emission. Gordon (1951), on the other hand, maintains that in uranyl nitrate solutions, particularly at room temperature, the UO_2^{++} ion does not fluoresce and the emission is due to the UO_2OH^+ ions. There are a great many other observations in literature on the behaviour of uranyl solutions but, as stated by Dieke and Duncan (1949), their significance for the understanding of the spectra of solutions is not clear. In a recent note (Pant and Khandelwal, 1957, 1959) specific attempts to investigate how exactly the fluorescence spectra are influenced by the presence of various chemical species in these solutions were reported. The present paper gives details of the results of studies made on uranyl nitrate solutions at room temperature.

The uranyl nitrate and other chemicals used were of A.R. grade. Conductivity water was used to prepare the solutions and pH was varied by addition of NaOH or HNO_3. No attempt was made to remove the dissolved oxygen from solutions. Absorption spectra were taken with the UVISPEK spectro-photometer and pH was measured with a Macbeth pH meter. Fluorescence spectra were recorded with a Bellingham Stanley monochromator and 931 A photomultiplier arrangement. The exciting radiation (3650 Å) from a 125-watt Philips black-light lamp, run on a constant voltage supply, was focussed by a large concave mirror with a central aperture so as to fall on the sample along the axis of the collimator, whereby more of the fluorescence light could be gathered by the monochromator and semiquantitative

estimates of relative fluorescence efficiencies could be made. Corrections for the spectral response of the photomultiplier and dispersion of the monochromator were applied to compare intensities in different spectral regions. The fluorescence curves given here, however, are drawn after the readings of the measurand only. Five to six bands could be observed in the spectra but the longer wavelength bands are not included owing to low sensitivity of the photomultiplier in that region. The curves were subjected to Gaussian analyses to get the positions and intensities of different bands. The bands are rather diffuse and their location may be in error by ± 5 Å. Values of integrated intensities are stated only for the bands in which the trends are systematic and of a degree far greater than possible errors in the analyses.

2. EXPERIMENTAL RESULTS

(*A*) *Absorption spectra.*—An extensive study of these spectra was made from 5000 Å to 2100 Å at concentrations between 2 M to ·001 M, pH < 1 to > 4 and NO_3^- concentration up to ~ 10 M. The general features of such spectra being well known, no details are presented. Briefly, on dilution (Fig. 1) the molar extinction coefficient ϵ decreases and reaches a minimum

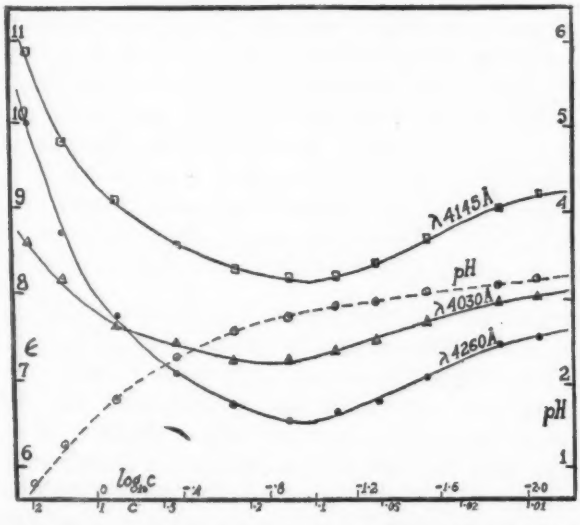

FIG. 1. Variation of ϵ at three of the bands in uranyl nitrate solution with variation of concentration (variation of pH is also shown).

of 8·2 at peak 4145 Å with concentration 0·1 M. It increases again on dilution. Even at the minimum, addition of slight acid (to lower pH < 2) reduced ϵ

to 7·8. Addition of alkali or acid to this solution increases ϵ. The absorption spectra of 0·1 M solution for various amounts of added HNO_3 are given along with one spectrum of alkaline solution in Fig. 2. The marked change at extreme NO_3^- concentration is to be noted.

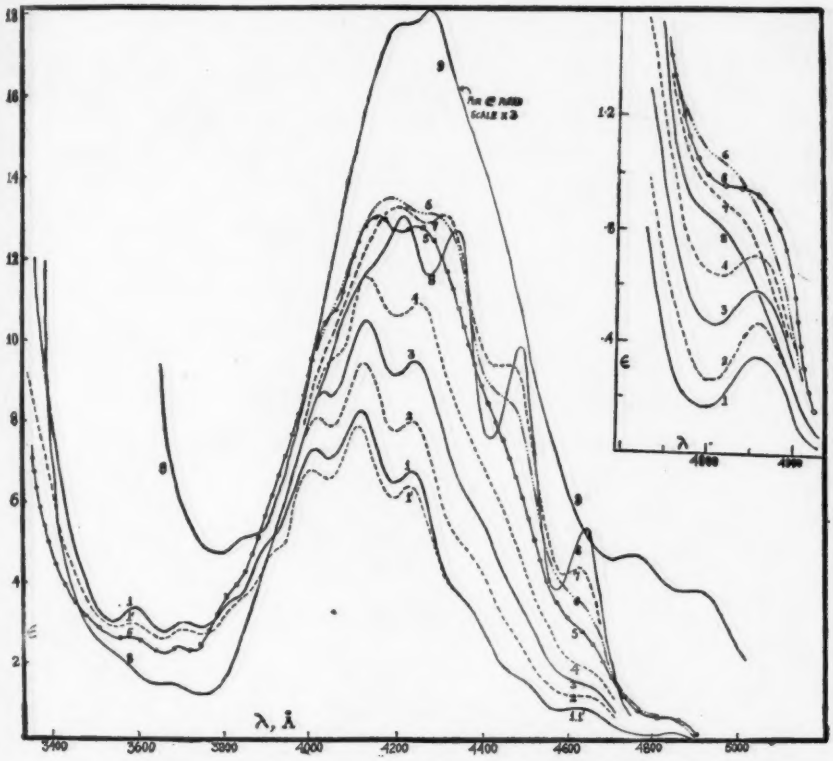

FIG. 2. Absorption spectrum of uranyl nitrate solution with varying quantity of nitric acid. U-concentration constant at 0·1 M; concentration of HNO_3 used: 68%. Proportion of HNO_3 by volume: (1) 0%, (1′) 5%, (2) 10%, (3) 15% (4) 25%, (5) 30%, (6) 40%, (7) 50%, (8) 100%. Curve 9 is for same solution with a little alkali (for comparison).

(*B*) *Fluorescence spectra.*—In Figs. 3 and 4 are shown some typical stages in the fluorescence spectra of aqueous solutions as the concentration varies from 2 M to 0·0015 M (pH ranging from 1·0 to 3·6). The effect of successive addition of nitric acid (68%) to a solution whose U-concentration was kept constant at 0·08 M is shown in Figs. 5 and 6. Figure 7 shows the effect of adding NaOH (0·002 M) to a 0·3 M solution. The spectrum of the solid hexahydrate is given in each figure for comparison. The

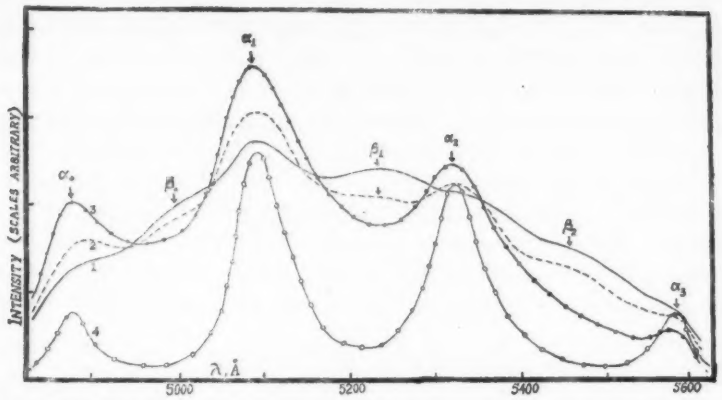

FIG. 3. Fluorescence spectrum of uranyl nitrate aqueous solution at room temperature with varying dilution. (1) 2 M, (2) 1 M, (3) 0·5 M, (4) spectrum of the solid nitrate (for comparison).

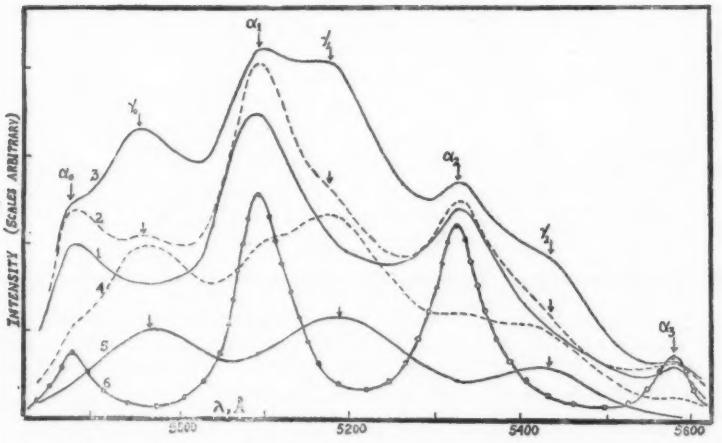

FIG. 4. Fluorescence spectrum of uranyl nitrate aqueous solution at room temperature with varying dilution (continued from Fig. 3). (1) 0·5 M, (2) 0·2 M, (3) 0·025 M, (4) 0·006 M, (5) 0·0015 M, (6) spectrum of the solid nitrate (for comparison).

positions of the various bands are given in Table I and relative integrated intensities of the different bands of two of the series in pure aqueous solutions are given in Table II.

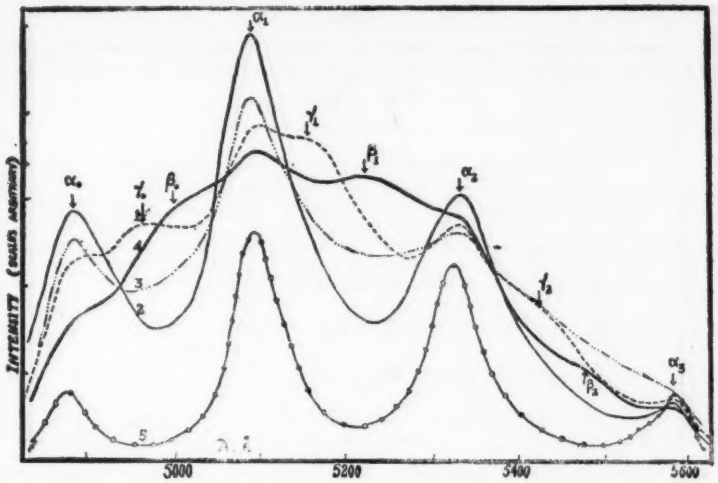

Fig. 5. Fluorescence spectrum of uranyl nitrate solution with varying quantity of nitric acid. U-concentration const nt at 0·08 M; concentration of HNO_3 used: 68%. Proportion of HNO_3 by volume: (1) 0%, (2) 0·1%, (3) 10%, (4) 30%, (5) spectrum of the solid nitrate (for comparison).

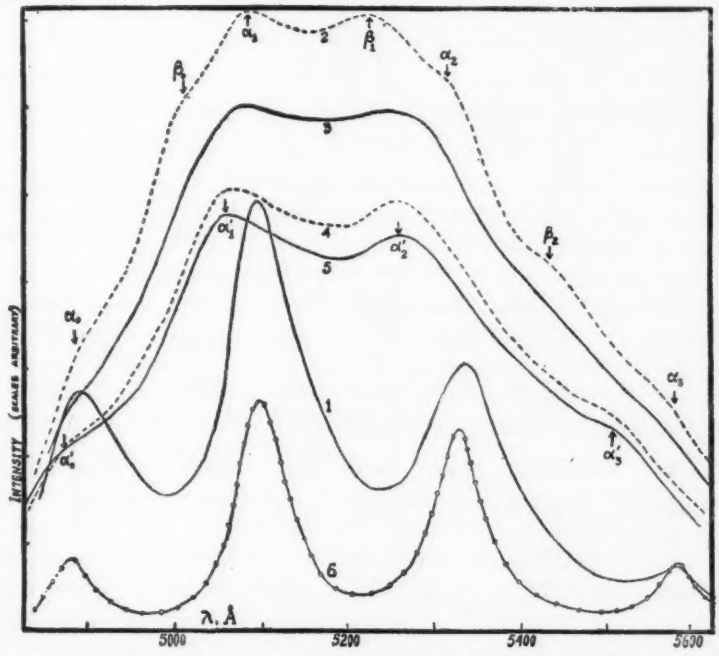

FIG. 6. Fluorescence spectrum of uranyl nitrate solution with varying quantity of nitric acid (continued from Fig. 5). Proportion of HNO_3 by volume: (1) 0·1%, (2) 30%, (3) 40% (4) 50%, (5) 75%, (6) spectrum of the solid nitrate (for comparison).

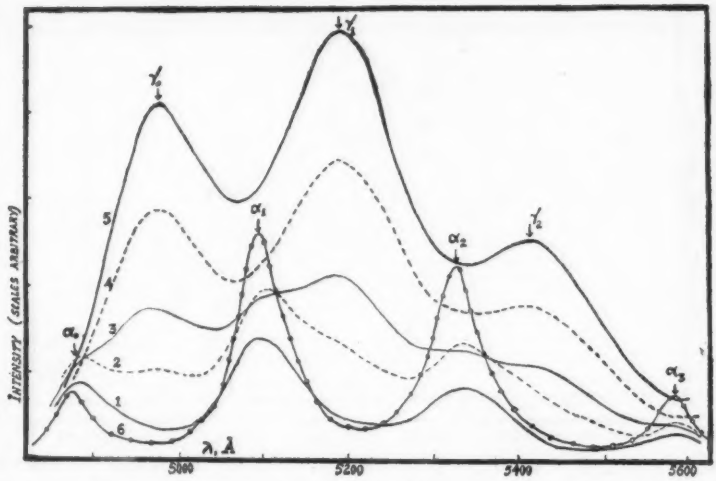

Fig. 7. Fluorescence spectrum of uranyl nitrate solution with varying quantity of NaOH. U-concentration constant at 0·3 M; NaOH used ~ ·002 M. (1) 0%, (2) 0·1%, (3) 0·3%, (4) 0·5%, (5) 1·0% NaOH by volume, (6) spectrum of the solid nitrate (for comparison).

TABLE I

Positions of various fluorescence bands at room temperature

Group		Bands of solution					Bands of solid	
		α	β	γ	α′	Levshin	Authors	N and H
0	λ Å ..	4888	5010	4970	4865	4879	4883	4882
	ν cm.$^{-1}$ ..	20453	19954	20115	20549	20490	20474	20478
1	λ Å ..	5108	5240	5185	5065	5100	5100	5096
	ν cm.$^{-1}$ ..	19572	19079	19281	19738	19602	19602	19618
2	λ Å ..	5350	5460	5420	5300	5340	5340	5331
	ν cm.$^{-1}$ ..	18686	18310	18445	18863	18721	18721	18753
3	λ Å ..	5610	..	..	..	5607	5590	5591
	ν cm.$^{-1}$ ..	17820	..	..	..	17830	17884	17886

TABLE II

Distribution of intensity between different fluorescence bands of α and γ series

Band	Intensity in solid	Intensity in solution						
		2 M	1 M	·5 M	·2 M	·025 M	·006 M	·0015 M
α_0 ..	0·28	0·38	0·44	0·45	0·49	0·54	0·52	..
α_1 ..	1·00	1·00	1·00	1·00	1·00	1·00	1·00	..
α_2 ..	0·76	0·46	0·53	0·69	0·70	0·77	0·83	..
α_3 ..	0·20	..	..	..	0·20	0·21	0·23	..
γ_0 ..					0·66	0·68	0·72	0·73
γ_1 ..					1·00	1·00	1·00	1·00
γ_2 ..					0·38	0·48	0·44	0·45

The following features are brought out by these studies:—

(i) The fluorescence spectrum of aqueous solutions of uranyl nitrate at room temperature can, under controlled conditions, exhibit four distinct series of bands, designated as α, β, γ and α' bands.

(ii) The concentrated solutions show α and β bands. With dilution the β bands diminish rapidly in intensity so that at 0·5 M only α bands are left. Dilute solutions show α and γ bands, the latter gaining in intensity with further dilution and appearing exclusively at great dilution. However, on increasing NO_3^- concentration by adding acid the β bands appear even in moderately dilute solution. The 0·08 M solution with 30% acid shows β bands fairly distinctly. On the other hand, when pH is increased by the addition of alkali even moderately concentrated solution show γ bands. For a 0·3 M solution $\sim$5% of ·002 M NaOH is enough to make the γ bands so strong as to suppress the α entirely.

The α' bands appear only in the extreme range of acidity (Fig. 6). In this range the β bands are not affected in intensity or position but the α bands shift towards the violet and tend to become indistinguishable, except in wavelength values, from the β bands. Ultimately at $\sim$75% acid content only a single set of bands (α') is present.

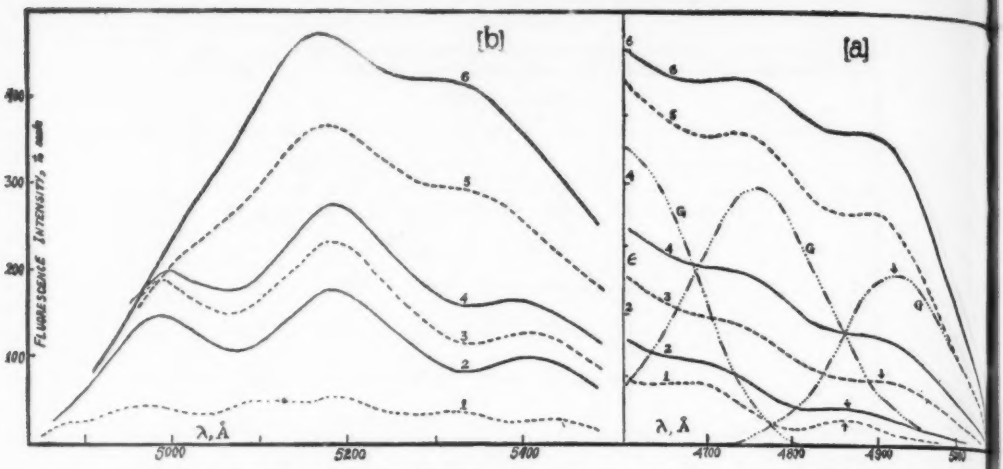

FIG. 8. (*a*) Absorption and (*b*) Fluorescence spectra of uranyl nitrate solution taken simultaneously with successive addition of NaOH, leading close up to a stage where precipitation would occur with further NaOH. U-concentration 0·08 M, Curves 1–6 are for successively increasing NaOH. (G) shows a Gaussian analysis of Curve 5 (*a*).

(iii) The α bands of solution are shifted with respect to the bands of the solid by ~ 30 cm.$^{-1}$ towards the red, but do not change in position with dilution or acid-alkali content. The β bands are shifted relatively to the corresponding α bands by an average of ~ 450 cm.$^{-1}$ towards red and the γ bands are similarly shifted by ~ 280 cm.$^{-1}$ The α' bands, on the other hand, lie to the violet of the corresponding α bands by ~ 170 cm.$^{-1}$

(iv) The frequency intervals in the β and α' series are, broadly speaking, the same as in α-series, *viz.*, 860 cm.$^{-1}$ The interval in γ series is less than in α-series.

(v) With dilution the overall intensity at first increases, but later on begins to fall. The fluorescence efficiency, however, increases continuously.

The intensity in the spectrum when the solution shows γ bands is much greater than in other cases. The spectrum is least intense when the α' bands are showing.

(vi) As regards intensity distribution the α bands in solution have their intensity shifted towards the (0, 0) band as compared to the bands of the solid. With dilution the intensity distribution gets wider (Table II).

The γ bands have a distribution far more shifted towards the (0, 0) band, so much so that this may be considered as one of the characteristics of these bands.

(vii) In structure the γ bands are less discrete than α bands. The β bands also have a structure more diffuse than that of α bands.

(*C*) *The* (0, 0) *bands in absorption corresponding to the different series.*— The first bands (Fig. 2) in the absorption spectra of aqueous solution (4860 Å) and of the highly acidic solution (4830 Å) obviously correspond to the α_0 (4888 Å) and α_0' (4865 Å) bands respectively in fluorescence. In search for an absorption band corresponding to γ series the absorption and fluorescence spectra were examined simultaneously for a ·08 M aqueous solution to which alkali was successively added. Figure 8 *a* shows that the first band in absorption shifts from 4860 Å to 4920 Å as ϵ at this band rises from 0·4 to 1·8. With further addition of alkali the band remains in an unchanged position at 4920 Å. This may therefore be taken as the (0, 0) absorption band corresponding to the γ_0 band (4970 Å) in fluorescence.

In Table III the separations of corresponding (0, 0) bands are given.

TABLE III

Separation of (0, 0) *bands in absorption and fluorescence*

Band	Absorption		Fluorescence		Separation
	λ, Å	ν, cm.$^{-1}$	λ, Å	ν, cm.$^{-1}$	$\Delta\nu$, cm.$^{-1}$
α_0 ..	4860	20570	4888	20453	117
α_0' ..	4830	20698	4865	20549	149
γ_0 ..	4920	20320	4970	20115	205

As regards absorption corresponding to the β bands, the situation is not clear. In the earlier stages of adding acid (up to 30%) where β bands develop in fluorescence (Fig. 6), the 4860 Å absorption band (Fig. 2) enhances in intensity but remains unchanged in position.

Curves 5 and 6 in Fig. 8 *b* show that when considerable alkali is added to the solution a distinct change in intensity distribution in fluorescence sets in. The intensity shifts towards the red, so that the longer wavelength bands become relatively more intense and the spectrum tends to become continuous.

3. DISCUSSION OF RESULTS

A considerable understanding of the chemistry of uranyl solutions has now been achieved by several physico-chemical studies (Sutton, 1949; Betts and Michels, 1949; Ahrland, 1951, 1954; Hearne and White, 1957; Robinson, Wilson and Ayling, 1942; Lipilina and Samilov, 1954). In dilute and acidic nitrate solutions (pH < 2) the ion exists as UO_2^{++}, possibly hydrated. In higher NO_3^- concentration range additional species like $UO_2NO_3^+$ will also be present, while at very high NO_3^- concentration Betts and Michels have indicated the possible formation of $UO_2(NO_3)_2$ also. On the other hand, in dilute solutions and/or large pH species like $UO_3UO_2^{++}$ are formed by hydrolysis:

$$(n+1)\,UO_2^{++} + n\,H_2O \rightleftharpoons (UO_3)_n\,UO_2^{++} + 2n\,H$$

Sutton, Betts and Michels have obtained ϵ values (at 4145 Å) for the separate species UO_2^{++}, $UO_3UO_2^{++}$ and $UO_2NO_3^+$ as 7·8, 67 and 15·5 respectively. Our studies of absorption spectra are largely in accord with these results and help us in identifying and estimating the particular species present in a given solution. Thus the 0·1 M aqueous solution has $\epsilon = 8{\cdot}2$ which falls to 7·8 on slight acidulation. This solution therefore contains predominantly the UO_2^{++} ions. On greater dilution or alkaline side ϵ increases due to the formation of the hydrolysed species $UO_2UO_3^{++}$, while on higher concentration or acidic side ϵ increases due to the formation of $UO_2NO_3^+$. In the extreme NO_3^- concentration range (Curve 8, Fig. 2) the sharp change in the spectrum is to be attributed to $UO_2(NO_3)_2$.

When the fluorescence results are seen in conjunction with the above conclusions the emitters of α, β, γ and α' bands are identified as UO_2^{++}, $UO_2NO_3^+$, $UO_3UO_2^{++}$ and $UO_2(NO_3)_2$ respectively. Since increase of pH enhances the γ series, the α bands cannot be due to a hydrolysed species like UO_2OH^+ as suggested by Gordon.

From the correspondence between the α bands of solution and the bands of the solid hexahydrate it would appear that the six molecules of water of crystallisation which octahedrally surround the uranyl ion in the solid may still be present in the solution in the same arrangement. This view of the hydrated UO_2^{++} ion is supported by entropy measurements of Coulter *et al.* (1940) and thermochemical investigations of Lipilina and Samilov (1954). However, differences arise between the spectra in the two cases due to environmental effects. The intensity distribution in bands of the solution is shifted towards the (0, 0) band and gets wider with increasing dilution. The first of these effects is obviously connected with the difference in the displacements of the potential minima of the ground and the excited states of the

ion in solution and solid. Raman spectra (Crandall, 1949; Sutton, 1952) do show slight deformation of the ion from linear structure in solution and this fact can account for the intensity shift. The second effect points to flattening of the electronic wave-functions of the vibrationless electronic states. Since the distance of approach of positive ion from the negative ions is independent of dilution (Gurney, 1953), there is no wavelength shift. However, with dilution long-range forces breakdown resulting in a minor widening of intensity distribution.

For the assignment of β bands quantitative considerations connected with absorption data also lend support. From ϵ values we get the proportion of $UO_2NO_3^+$ to UO_2^{++} in 2 M, 1 M and ·5 M solutions as ·75, ·35 and ·15 respectively. Now, considering that the ϵ for the two species at 3650 Å (exciting radiation) are 2·0 and 3·5 respectively the intensity ratios β/α in the solutions should be ·43, ·20 and ·086. The actual values ·49, ·24 and ·10 are in surprisingly good agreement with the calculated values, particularly in view of the complicated quenching processes connected with dilution.

As regards γ bands a notable fact is that they make their appearance to the entire exclusion of α bands even when the proportion of $UO_3UO_2^{++}$, as calculated from absorption data, is very small. For example, in the case of a ·08 M aqueous solution calculation shows that the $UO_3UO_2^{++}$ species is only 0·8%. Accounting for the fact that ϵ value for this species at 3650 Å is 10 times that for the UO_2^{++} ion, the γ to α intensity ratio in fluorescence should have been 1 : 12. The corresponding fluorescence curve, on the other hand, shows the γ bands at least as prominently as the α bands. This shows that either the species $UO_3UO_2^{++}$ is better shielded from deactivating collisions and has consequently higher fluorescence efficiency, or the UO_2^{++} ion itself is transferring its energy to this ion. The latter possibility cannot be discarded, especially in view of the fact that the excited state of $UO_3UO_2^{++}$ is energetically lower than that of UO_2^{++} (the difference is $\sim$ ·05 eV.).

The possibility of explaining the γ bands as due to a vibrational frequency of ~ 340 cm.$^{-1}$ is ruled out because no such frequency is observed in absorption and because the (0, 0) band in absorption due to $UO_3UO_2^{++}$ is definitely obtained. Although there is a rather large shift between the (0, 0) band in fluorescence and absorption (~ 200 cm.$^{-1}$), yet this shift is observed in α series as well. Such relative shifts are well known in the condensed state spectra (Garner, 1955).

The change in the nature of the spectrum at later stages of addition of alkali (Fig. 8 *b*) points to the formation of more complex hydrolysed species,

e.g., $(UO_3)_2\,UO_2^{++}$, etc. This development comes about at almost the same pH value at which Sutton reports it from absorption experiments in perchlorate solution. However, the change is far more marked in the fluorecence spectrum than in absorption.

It is interesting to recall that the spectra of hydrated UO_3 in the solid state (Dieke and Duncan, *loc. cit.*) resemble the γ bands reported here. Compared to the solid nitrate, in both the cases the bands are more diffuse, the intensity distribution is shifted very conspicuously towards the (0, 0) band, the spectra are shifted towards the red and the vibrational frequency is decreased. Now, in the trioxide each uranium atom has two nearest 0 atoms at 2·08 Å compared to 1·19 Å in the uranyl ion (Zachariasen, 1948). The electronic energy difference between the excited and the ground state and the vibrational frequency are $19{\cdot}7\times10^{-3}$ cm.$^{-1}$ and 810 cm.$^{-1}$ in hydrated UO_3 as compared to $20{\cdot}5\times10^{-3}$ cm.$^{-1}$ and 860 cm.$^{-1}$ respectively in uranyl nitrate. These differences may be attributed to the repulsion of the uranyl oxygens by other oxygen atoms in UO_3 and consequent decrease in force constant. Apparently, in the hydrolysed species too the interatomic distances and force constants are influenced markedly by the extra oxygen atoms.

The authors wish to thank Prof. R. K. Asundi for useful discussions.

4. SUMMARY

The fluorescence spectra of uranyl nitrate solutions at room temperature are shown to give four distinct series of bands, designated α, β, γ and α', depending upon concentration, pH, etc. The α, β and γ series are respectively shown to be probably due to the species UO_2^{++}, $UO_2NO_3^{+}$ and $UO_3UO_2^{++}$. Higher hydrolysed species, when present, shift the spectrum towards the red. The species have been identified with the help of absorption spectra and their comparison with the results of earlier workers. α' bands are probably due to a species of the type $UO_2\,(NO_3)_2$. The intensity distribution in the various series is studied and it is found that in α and γ bands the intensity distribution gets wider on dilution. The various characteristics observed as regards the bahaviour of the different series are discussed on the basis of environmental differences of the species in the solid and solution states. A close resemblance between the spectra of hydrated solid UO_3 and γ bands is pointed out.

REFERENCES

1. Ahrland .. *Acta Chem. Scand.*, 1951, **5**, 1151, 1271: 1953, **7**, 485.
2. ——, Heitanen and Sillin .. *Ibid.*, 1954, **8**, 1907.
3. Betts and Michels .. *J. Chem. Soc.*, 1949, Suppl. 2, 286.

4. Coulter, Pitzer and Latimer .. *J. Am. Chem. Soc.*, 1940, **62**, 2845.
5. Crandall .. *J. Chem. Phys.*, 1949, **17**, 602.
6. Dieke and Duncàn .. *Spectroscopic Properties of Uranium Compounds*, McGraw-Hill, 1949.
7. Garner .. *Chemistry of the Solid State*, Butterworths, 1955.
8. Gordon .. *Izvest. Akad. Nauk. U.S.S.R. Ser., Fiz.*, 1951, **15**, 124.
9. Gurney .. *Ionic Processes in Solution*, Mc-Graw-Hill, 1953.
10. Hearne and White .. *J. Chem. Soc.*, 1957, 2168.
11. Levshin .. *Acta Physicochim., U.S.S.R.*, 1937, **6**, 661.
12. Lipilina and Samilov .. *Doklady Akad. Nauk S.S.S.R.*, 1954, **98**, 99.
13. Nichols and Howes .. *Flourescence of Uranyl Salts*, Carnegie Inst. Wash., 1919, 180–225.
14. Pant and Khandelwal .. *Curr. Sci.*, 1957, **26**, 282; *J.S.I.R.*, 1959, **18 B**, 126.
15. Pringsheim .. *Fluorescence and Phosphorescence*, Interscience, 1949.
16. Robinson, Wilson and Ayling *J. Am. Chem. Soc.*, 1942, **64**, 1479.
17. Sutton .. *J. Chem. Soc.*, 1949, Suppl. 2, S 275.
18. ———— .. *Nature*, 1952, **169**, 235.
19. Zachariasen .. *Acta Cryst.*, 1948, **1**, 265.

STUDIES ON METALLIC HALIDE DIOXANATES

II. Dioxanates of Cupric and Ferric Chlorides

By S. G. K. Nair and S. S. Moosath

(Applied Chemistry Department, University of Kerala, Trivandrum)

Received July 7, 1959

(Communicated by Dr. M. R. A. Rao, F.A.SC.)

Introduction

Molecular addition compounds of metallic halides with several ethers have been extensively studied and dioxanates of several metallic halides are reported.[1–6] Rheindboldt *et al.*[7] in the course of their systematic investigations of the dioxane complexes of the halides of mono-, di- and trivalent metals have reported cupric chloride dioxanate with the formula $CuCl_2 \cdot C_4H_8O_2$ as a relatively unstable compound. Later studies by Virginia *et al.*[8] have shown that cupric chloride forms a di-dioxanate. The method of preparation followed by the earlier workers is the direct mixing of dioxane and the metallic halide and subsequent purification. In view of the reported differences in the composition of cupric chloride dioxanate and in view of the absence of any previous studies on ferric chloride dioxanate, the present investigations have been made by the authors. The new method developed by the present authors[9] for the preparation of mercuric chloride dioxanate is employed for the isolation of the dioxanates described in this paper.

The freshly prepared dry metallic oxide or hydrous oxide is suspended in pure dry dioxane and treated with dry hydrogen chloride gas. The hot solution is filtered under dry conditions to remove unreacted or hydrolysed materials and the filtrate is cooled overnight at 0° C. when crystals of the dioxanate separate. The crystals are collected in a dry sintered funnel, washed with dry petroleum ether and treated with a current of dry air. The samples if necessary can be recrystallised from dioxane. The pure samples are then analysed for metal and chloride.

Discussion

Cupric chloride dioxanate thus prepared and analysed is found to be the mono-dioxanate, the analytical values agreeing with the formula $CuCl_2 \cdot C_4H_8O_2$. Cupric chloride dioxanate is very sparingly soluble in

dioxan and this fact makes the method of preparation less convenient and efficient. On treatment with hydrogen chloride gas, a brownish product gets precipitated, covering the unreacted copper oxide and thus preventing completion of the reaction. This difficulty is observed with precipitated copper oxide and to a larger measure with ignited oxide, but when cupric hydroxide dried to constant weight at 160° C. is used, a homogeneous product is obtained. Solubility of the complex in dioxane is considerably low and only a small quantity of the crystals could be obtained on cooling the filtrate. The crystals are brownish in colour, needle-shaped and highly hygroscopic. On exposure to air, the colour changes to bluish green. The complex is very soluble in water, the concentrated solution becoming blue. The dioxanate is very stable and remains unchanged even after heating to 140° C. or after evacuation at 1 mm. pressure for 2 hours. No change in composition occurs when crystallised from alcohol. But when crystallised from water the dioxanate is destroyed and cupric chloride dihydrate is obtained. At no stage in the present investigations, the authors were able to get the didioxanate of cupric chloride as reported by Virginia *et al.*

Ferric chloride is found to form the tridioxanate with the formula $FeCl_3 \cdot 3\ C_4H_8O_2$. Trivalent halides of arsenic, antimony and bismuth form molecular addition compounds with dioxane[10] with the general formula $2\ MCl_3 \cdot 3\ C_4H_8O_2$ (where M = As; Sb or Bi) and aluminium halides form both mono- and didioxanates.[11] Among the transition elements, Cobalt is reported to form $CoI_3 \cdot 3\ C_4H_8O_2$; $CoI_3 \cdot 2\ C_4H_8O_2$ and $CoI_3 \cdot C_4H_8O_2$. Ferric chloride shows close resemblance to cobalt iodide in the number and stabilities of their dioxanates. The present method of preparation is highly suitable for isolating ferric chloride dioxanate. Both hydrous and ignited ferric oxides are found to be equally good as starting material. Ferric oxide suspended in dioxane is rapidly and vigorously attacked by hydrogen chloride gas. No unreacted oxide remains and no ferric chloride complex gets precipitated. However, the solubility of the complex in dioxane is so high that the yield on crystallisation is small. The dioxanate is obtained as pale green thin plates. It is extremely hygroscopic and changes to an yellowish brown viscous liquid on exposure to air. The crystals can be best preserved in petroleum ether or in an atmosphere of dioxane vapour . When kept in a desiccator, slow changes in colour and crystalline form set in, with loss of dioxane. A product approximating to the composition $2\ FeCl_3 \cdot 3\ C_4H_8O_2$ can be obtained by crystallisation of the tridioxanate from alcohol. When kept in a vacuum, the tridioxanate slowly changes to give first $2\ FeCl_3 \cdot 3\ C_4H_8O_2$ and finally $FeCl_3 \cdot C_4H_8O_2$. The monodioxanate can be obtained within 90 minutes if the evacuation is done at 110° C. The

dioxanate is more highly soluble than ferric chloride itself in alcohol and acetone. However, the acetone solution undergoes colour change and slow decomposition even at 0° C.

EXPERIMENTAL

Materials Used

(1) *Cupric oxide.*—(*a*) A.R. grade copper sulphate (50 g.) was dissolved in water and a dilute solution of sodium hydroxide added till precipitation was complete. The precipitate was allowed to stand at 80° C. for one hour, filtered and washed free of soluble impurities. It was then dried at 160° C. to constant weight, powdered and stored. Analysis of the sample showed it to be pure cupric oxide.

(*b*) A.R. grade copper carbonate (25 g.) was ignited in a platinum dish at 800° C. The copper oxide thus obtained was cooled and stored.

(*c*) A.R. grade copper sulphate (50 g.) was dissolved in water and 1 N ammonium hydroxide was added in drops till precipitation was complete. The precipitated cupric hydroxide was filtered off, washed free of sulphate and dried at 160° C. to constant weight.

Ferric oxide.—(*a*) A.R. grade ferric ammonium sulphate (100 g.) was dissolved in water and 1 N ammonium hydroxide added to precipitate the ferric hydroxide. The precipitate was filtered off, washed free of sulphate and dried at 160° C. to constant weight.

(*b*) The hydrated ferric oxide (10 g.) prepared as in (*a*) was ignited at 900° C. cooled and stored.

Dioxane.—C.P. grade B.D.H. make dioxan was refluxed with sodium, distilled and stored over sodium wire.

Dry hydrogen chloride gas was prepared as and when required.

Analytical.—Pure samples of the dioxanates were analyesd for metal and chloride by standard methods.

Preparation of Cupric Chloride Dioxanate

Cupric oxide (5 g.) sample (*a*) was suspended in dioxan (200 ml.) and treated with dry hydrogen chloride gas. The contents of the vessel were cooled in cold water. A brown product was formed which got mixed up with the unreacted cupric oxide. As the reaction proceeded, the amount of the brown product increased, but even after one hour some cupric oxide was found to remain. The contents of the vessel were filtered under dry

conditions and the filtrate let stand overnight at 0° C. Light brown needle-shaped crystals of the dioxanate separated at the bottom of the vessel. The crystals were collected on a dry sintered funnel, washed with petroleum ether, dried in a current of dry air and analysed for copper and chloride. Found: per cent., Cu: 28·34; Cl: 31·98. Calculated per cent. values for the formula $CuCl_2 \cdot C_4H_8O_2$: Cu: 28·56; Cl: 31·86. Most of the dioxanate formed by the reaction was admixed with unreacted copper oxide. When the ignited copper oxide, sample (*b*) was used in the above reaction, the behaviour was nearly identical, except that the reaction was slower and the amount of unreacted oxide was larger. But when cupric hydroxide sample (*c*) was made to react, the entire copper reacted rapidly and a brownish homogeneous product was obtained. This product after washing with petroleum ether was analysed. Found : per cent., Cu: 28·85; Cl: 31·21. Because of the very low solubility in dioxane, it could not be recrystallised successfully. The filtrate after removal of the brownish product gave, on cooling, needle-shaped crystals of the dioxanate $CuCl_2 \cdot C_4H_8O_2$.

Stability studies.—(1) The crystals on heating in a melting point tube underwent slight colour change to greyish brown at 140° C. There was no noticeable change till 300° C. and on further heating the substance charred leaving a black residue. The dioxanate was found to remain unchanged for several weeks when kept in a dry atmosphere. Evacuation at room temperature at 1 mm. pressure for two hours did not bring about any change in composition.

(2) *Effect of crystallising from water.*—A saturated solution of the dioxanate in water was prepared at 60° C. and the clear solution kept overnight at 0° C. Bluish green crystals that separated were removed, dried between folds of filter-paper and analysed. Found: per cent., Cu: 37·03; Cl: 41·14. Calculated per cent. values for the formula $CuCl_2 \cdot 2H_2O$: Cu: 37·26; Cl: 41·58.

From alcohol.—The dioxanate is fairly soluble in alcohol, the solution acquiring an olive green colour which becomes deeper with concentration. A saturated solution of the dioxanate crystals in about 50 ml. absolute alcohol was prepared at 40° C. and the clear solution cooled to 0° C. A solid phase got separated after two days, as hard plates with brick-red colour. However, the solid on analysis gave the same values as the original dioxanate. The crystallised product was heated under vacuum for two hours and there was no loss in weight showing that it was a very stable compound.

From acetone.—Cupric chloride dioxanate is only very sparingly soluble in acetone, the solution acquiring a pale brownish colour. A product with definite crystalline shape or composition could not be isolated.

Preparation of Ferric Chloride Dioxanate

The procedure adopted was the same as described earlier. Ferric oxide (5 g.), sample (*a*) suspended in 100 ml. dioxane was treated with hydrogen chloride gas. The reaction was very fast and a dull green clear solution was obtained within fifteen minutes. All the ferric oxide had gone into solution and the complex had not precipitated during the reaction. The solution was kept overnight at 0° C. when the dioxanate separated. The crystals were transferred to a sintered funnel, washed several times with petroleum ether and kept in a current of dry air for 30 minutes. The sample was then analysed for iron and chloride. Found: per cent., Fe: 13·22; Cl: 25·15. Calculated per cent. values for the formula $FeCl_3 \cdot 3C_4H_8O_2$: Fe: 13·10; Cl: 24·97.

The experiment was then repeated with ignited ferric oxide (sample *b*). Reaction proceeded in almost identical manner except for the slower rate and the same product was obtained.

Stability studies.—Ferric chloride tridioxanate even on keeping under dry conditions is found to be unstable. In about 10–12 days it becomes black and sticky. However, it can be preserved indefinitely under petroleum ether. When exposed to air, it rapidly absorbs moisture and behaves like ferric chloride. It is readily soluble in water, at first giving an yellowish green solution which on keeping becomes more yellow and finally yellowish-brown, possibly due to hydrolysis and formation of colloidal ferric hydroxide.

The dioxanate dissolves readily in alcohol imparting a pale yellow colour to the solution. Even after cooling a saturated solution to — 20° C., only a small amount of the crystals could be obtained. Analysis of this product does not give any concordant results, but the values approximate for the formula $2FeCl_3 \cdot 3C_4H_8O_2$.

The dioxanate crystals are equally highly soluble in acetone, the solution becoming pale brown in colour. But within 30 minutes, even at 0° C. the colour was found to deepen and in two hours, the solution became dark brown in colour. On cooling to —20° C., a dark brown solid got deposited, together with a tarry oily matter on the top of the solution. Attempts to identify the products were unsuccessful.

The dioxanate crystals, on slowly heating with a naked flame, melt and then burn with a smoky flame. On stronger heating ferric oxide is obtained. When kept in a vacuum there was progressive loss in dioxane and two lower dioxanates $2\,FeCl_3 \cdot 3\,C_4H_8O_2$ and $FeCl_3 \cdot C_4H_8O_2$ could be isolated. These lower dioxanates are more stable than the tridioxanate, the monodioxanate being most stable.

Summary

Cupric chloride dioxanate has been prepared by the new method developed by the authors and shown to be the monodioxanate. Stability studies and effects of crystallisation from different solvents are reported.

The tridioxanate of ferric chloride is prepared and studied. Existence of two lower dioxanates of ferric chloride has been indicated.

References

1. Crenshaw, J. L., *et al.* .. *J. Amer. Chem. Soc.*, 1938, **60**, 2308.
2. Curran, W. J. and Wenzke, H. H. *Ibid.*, 1935, **57**, 2162.
3. Mecusker, P. A. and Curran, W. J. *Ibid.*, 1942, **64**, 614.
4. Hamilton, P. M., *et al.* .. *Ibid.*, 1953, **75**, 2881.
5. Rolston, R. F, and Sisler, H. H. *Ibid.*, 1957, **79**, 1068.
6. ——— .. *Ibid.*, 1957, **79**, 1819.
7. Rheindboldt, H., *et al.* .. *J. Prakt. Chem.*, 1937, **148**, 81; *Ibid.*, 1937, **149**, 30.
8. Virginia, A., *et al.* .. *Trans. Kentucky. Acad. Sci.*, 1938, **7**, 85.
9. Nair, S. G. K. and Moosath, S. S. *Proc. Ind. Acad. Sci.*, 1958, **47**, 344.
10. Kelley, C. J. and McCusker, P. A. .. *J. Amer. Chem. Soc.*, 1943, **65**, 1307.
11. Sheka, I. A. .. *Zhur. Obshchei, Khim. J. Jen. Chem.*, 1951, **21**, 833.

DECAY OF Eu^{155}

By Kumari S. Y. Ambiye, M. C. Joshi and B. V. Thosar, F.A.Sc.

(*Tata Institute of Fundamental Research, Bombay*)

Received July 13, 1959

Introduction

Europium^{155} is known[1] to decay to Gadolinium^{155} with half life about 1·7 years. There are three decay schemes proposed recently, one by Dubey *et al.*,[2] the other by Juliano[3] and the third by Bisi and Zappa.[4] The last two decay schemes are similar except that there is one more level at 117 kev. to explain new transitions observed by them. There is considerable disagreement about spin and parity assignments to these levels and also about the β-groups. Since Gd^{155} is an odd A nucleus in the region of nuclei where large deformation is known to be present, it would be interesting to know more about these nuclear levels. This isotope was reinvestigated using intermediate image Siegbahn-Slätis β-ray spectrometer adapted for β-$\bar{e}$-coincidence measurements. The conversion line spectrum of this isotope has not been studied so far using this technique.

Observations

The source was obtained by irradiating in Oak Ridge Pile, a sample of Sm^{154}, enriched to 99·1%. The other activity produced was due to Eu^{156} which decays to Gd^{156} with half life of 15 days. About a year had elapsed before the observations on Eu^{155} were started. There was thus no possibility of Eu^{156} being present in appreciable amount. Other impurity that was observed was Eu^{154}. Contribution due to Eu^{154} could easily be established by coincidence measurements as shown later.

(*a*) The spectrometer was adjusted for resolution 2·7% as tested with Cs^{137} source of 3 mm. diameter. Eu^{155} source was prepared by evaporating a drop of solution on a thin plastic film made conducting by aquadaq. Insuline was used for getting uniform sources. The β-particle detector on the focussing side was a thin anthracene crystal covered with 150 μgm./cm.^{2} thick aluminium foil as a reflector, and mounted on a perspex light guide, 9″ long and 1″ diameter, which passes through the pole piece of the spectrometer. EM.I. photomultiplier tube 6260 type was used. Pulses from the anode were fed to the amplifier and discriminator and to the recorder. The

low energy response was tested with K and L lines of 84 kev. transition in the decay of Tm^{170}. Performance of this scintillation detector was tested by studying different well-known isotopes (*e.g.*, Co^{60}, Tm^{170}, Ce^{144} and Eu^{152}). One finds only three distinct peaks superposed on very intense background due to β-continuum. These conversion lines have been identified as due to 86 kev. ($K_1 L_1$) and 105 kev. ($K_2 L_2$) transitions. An estimate of relative intensities of these lines based on such a spectrum would be in great error. From the spectrum it appears that there is a high energy β-group which extends up to about 1,800 kev. Fermi analysis showed the presence of two main high energy β-groups, $\beta_a \triangleq 1{,}800$ kev. and $\beta_b \triangleq 830$ kev. which were attributed to Eu^{154}. Fermi analysis of low energy β-spectrum after subtracting above-mentioned high energy β-groups reveals the other β-groups as follows:—

β-Groups	Energy	Intensity	log (ft.)
β_1	.. 245 ± 5 kev.	20%	8·1
β_2	.. 182 ± 5 kev.	22%	7·7
β_3	.. 145 ± 5 kev.	58%	7·1

E. L. Church[3] finds the following β-groups: $\beta_1 = 250$; $\beta_2 = 190$; $\beta_3 = 160$ and $\beta_4 = 150$ kev. It has not been possible to resolve the last two β-groups.

(*b*) A plastic scintillator $\frac{1}{8}''$ thick, $\frac{3}{4}''$ diameter was kept behind the source for detecting the β-particles. Discriminator level was kept sufficiently low to admit the pulses due to low energy electrons also. Pulses from the discriminator, on both sides, were fed to a coincidence unit with resolution, 0·25 μsec. Performance of the coincidence unit was tested with a Tm^{170} source. Only K and L conversion peaks due to 84 kev. transition were observed in coincidence with β-rays and the background due to the β-spectrum was completely suppressed.

Figure 1 shows the conversion electron spectrum in coincidence with β-rays in the decay of Eu^{155}. This spectrum reveals several conversion lines. They have been identified as due to γ_1 (86 ± 2 kev.); γ_2 (104 ± 2 kev.); γ_3 (31 ± 2 kev.); γ_4 (38 ± 2 kev.) and γ_a (120 ± 2 kev.). The interpretation of the lines observed is given in Table I.

The transition energies given in the last column are mean values obtained in different runs. Our observation confirms the presence of γ-rays of about 30 kev. and 39 kev. energy reported by Bisi for the first time from his γ-γ coincidence observations. The γ-ray of energy 60 kev. reported by

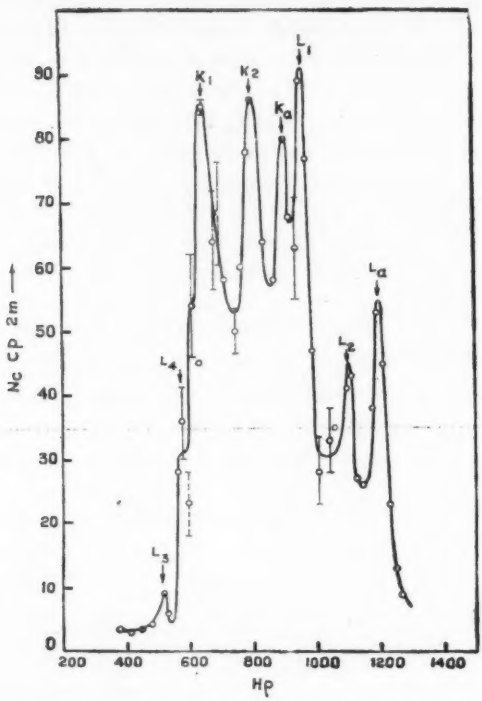

FIG. 1. Conversion electron spectrum in coincidence with β-rays, for Eu^{155}.

TABLE I

Line energy	Identity	Energy of the transition
23 kev. ..	L_3	31 $\pm$ 2 kev. (γ_3)
28·5 kev. ..	L_4	38 $\pm$ 2 kev. (γ_4)
36·5 kev. ..	K_1	86 $\pm$ 2 kev. (γ_1)
54 kev. ..	K_2	104 $\pm$ 2 kev. (γ_2)
68·5 kev. ..	K_a	120 $\pm$ 2 kev. (γ_a)
77 kev. ..	L_1	..
97·5 kev. ..	L_2	..
114 kev. ..	L_a	..

others[1, 3, 5] has not been resolved. L-shell conversion line energy of this transition is 51·63 kev. which overlaps the K-conversion line energy of 104 kev. transition at 53·7 kev. The K-shell conversion line due to 60 kev. transition and L-conversion line due to 18 kev. transition reported by some others[1, 3, 5] are too low in energy to be detected in the present arrangement. Another weak transition of energy 45 kev. has been reported by Boehm but not by others. However, it was not possible to observe it here since its L-conversion line falls very close to the K-conversion line of 86 kev. transition. Since the reported conversion line intensity of this transition is only about 5% that of 86 kev. transition its contribution in estimating K/L + M ratio for 86 kev. transition has been neglected, this being within the statistical errors. Using the theoretical value for L/M ratio (M. E. Rose[6]) the ratio K/L was calculated to be $2{\cdot}6 \pm 0{\cdot}6$.

Since a weak high energy β-group was observed in the β-spectrum and which was attributed to Eu^{154} impurity it was necessary to find if there are any conversion lines observed belonging to Eu^{154}. By adjusting the discriminator level, low energy β-groups were cut off and conversion line spectrum in coincidence with high energy β-rays was studied in the same region. Only two conversion lines (Ka and La, Fig. 2) were observed. These two

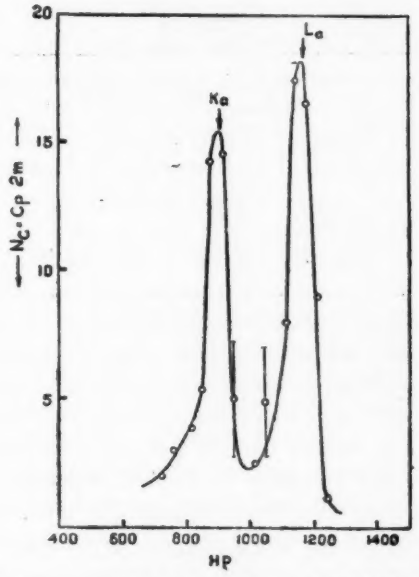

FIG. 2. Conversion electron spectrum in coincidence with high energy β-rays.

lines were interpreted as due to 122 kev. transition in the decay of Eu^{154}. The K/L ratio for this transition was found to be about 1·0 which is in agreement with the value reported by other observers.[7] This reveals the usefulness of this technique.

RESULTS AND DISCUSSION

From the internal conversion spectrum taken in coincidence with β-particles the K/L ratio was determined for the 86 and 104 kev. transitions as $2{\cdot}6 \pm 0{\cdot}6$ and < 6 respectively. Only the upper limit has been given for 104 kev. transition because the contribution of L-line of 60 kev. transition could not be determined. Rutledge[8] finds K/L ratio for the 86 kev. transition as 8 whereas Lee and Katz find it to be ~ 4. Lee and Katz[9] observe another transition of energy about 130 kev. The K-line of this transition falls very close to the L-line of 86 kev. transition. These could not be resolved in our spectrometer. This can result in giving a lower value for K/L ratio for the 86 kev. transition. But Church and Goldhaber[10] pointed out that 130 kev. γ-ray may be due to Eu^{150} impurity which was however not present appreciably in our sample. Comparing the K/L ratio with the theoretical values (Table II) corrected for finite nuclear size it is concluded that this is $E_2 + M_1$ transition, whereas 104 kev. transition may be $(E_1 + M_2)$ or $(E_2 + M_1)$ transition.

TABLE II

Transition	Theoretical K/L ratio				Experiment
Energy	E_1	E_2	M_1	M_2	K/L
86 kev. ..	6·7	0·8	7·9	3·3	$2{\cdot}6 \pm 0{\cdot}6$
104 kev. ..	6·92	1·06	7·6	3·7	< 6

Juliano observes $L_I : L_{II} : L_{III}$ from visual intensity measurement with high resolution spectrograph as medium : very medium : weak medium and he concludes that 86 kev. transition is E_1 type. Our value for K/L ratio favours $E_2 + M_1$ type of transition. Based on these observations as well as those of others a new decay scheme for Eu^{155} is proposed (Fig. 3). This decay scheme is similar to the one proposed by Bisi in which a new level at 117 kev. is assumed to explain 87 kev. and 30 kev. transition in cascade.

There is no arrangement about the spin assignments made by different workers. The spin of the ground state of Gd^{155} has been measured by Jenkins

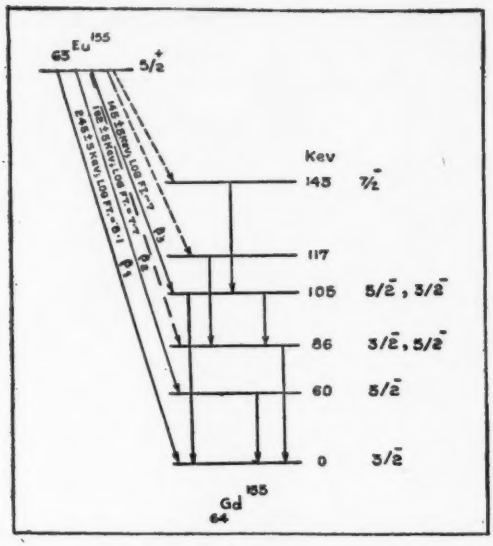

FIG. 3. Decay scheme of Eu^{155}.

and Speck[11] as 3/2 and by Murakawa[12] as $\geqslant 5/2$. Dubey and others assign $7/2^-$ for the ground state, $9/2^-$ for the 18 kev. state and $5/2^-$ for the 102 kev. state to get a better spin sequence on the basis of the shell model. Accordingly 84 kev. is mainly E_2 type and 104 kev. transition is $E_2 + M_1$ type, which is in agreement with our observations. The ground state ($3/2^-$), 60 kev. ($5/2^-$) and 144 kev. ($7/2^-$) states are known to belong to one rotational level.[13] It is not possible to make definite spin assignment to all the other states. Assignment of spin $3/2^-$ or $5/2^-$ to 86 kev. level and $5/2^-$ or $3/2^-$ to 105 kev. level has been made on the basis of our experimental observations of K/L ratio and log *ft* values. Spins $3/2^+$ for 86 kev. level and $5/2^+$ for 105 kev. level have been assigned by Juliano. This would mean the 145 kev. β-transition ($5/2^+ \rightarrow 5/2^+$) is of allowed type. But log *ft* value is about 7·1 which favours 1st forbidden type of β-transition ($5/2^+ \rightarrow 5/2^-$) in agreement with our assignment.

Our thanks are due to Shri S. D. Bhagwat and Shri C. V. Panat for their kind help during this work.

SUMMARY

Decay of Eu^{155} has been studied using intermediate image β-ray spectrometer, modified to make β-$\bar{e}$ and β-γ coincidence measurements.

The following β-groups have been observed: 245 kev., 182 kev. and 145 kev. K/L ratio for 86 kev. transition is found to be $\sim 2 \cdot 6$. A decay scheme has been proposed.

REFERENCES

1. Stromiger, D., Hollander, J. M. and Seaborg, G. T. — *Rev. Mod. Phys.*, 1958, **30**, Part II.
2. Dubey, V. S., Mandeville, C.E. and Rothman, M.A. — *Phys. Rev.*, 1956, **103**, 1430.
3. Juliano, J. O. .. — *Univ. California Radiation Lab. J. Rept. U.C.R.L.*-3733.
4. Bisi, A. and Zappa, L. .. — *Nucl. Phys.*, 1958, **6**, 252.
5. Boehm, F. and Hateh, E. N. — *Bull. Am. Phys. Soc.*, 1957, **2**(4), 231 W_3.
6. Rose, M. E. .. — *Table of Internal Conversion Coefficients*, North-Holland Publishing Co., Amsterdam, 1958.
7. Cork, J. M., Brice, M. K. Helmer, R. G. and Sarason, D. E. — *Phys. Rev.*, 1957, **107**, 1621.
8. Rutledge, W. C., Cork, J. M. and Burson, S. B. — *Ibid.*, 1952, **86**, 775.
9. Lee, M. R. and Katz, R. .. — *Ibid.*, 1954, **93**, 155.
10. Church, E. L. and Goldhaber, M. — *Ibid.*, 1954, **95**, 626 A.
11. Speck, D. R. and Jenkins, F. A. — *Ibid.*, 1956, **101**, 1725.
12. Murakawa, K. .. — *Ibid.*, 1954, **96**, 1544.
13. Heydenburg, N. P. and Temmer, G. M. — *Ibid.*, 1956, **104**, 981.

1073–59 Printed at the Bangalore Press, Bangalore City, by C. Vasudeva Rao, Superintendent and Published by The Indian Academy of Sciences, Bangalore

NOTICE TO AUTHORS

Scientific papers intended for publication in the *Proceedings of the Indian Academy of Sciences* can be accepted only when they are communicated by a Fellow of the Academy whose duty shall be to satisfy himself that such communications are fit to be read at the Meeting of the Academy and published in its *Proceedings*.

Papers should not ordinarily exceed fifty pages of foolscap. MSS. should be either typewritten or written in legible hand on one side of the paper. All papers should be carefully revised by the authors and should be absolutely in final form for printing. Position for text-figures should be indicated. Each paper shall conclude with a critical summary not exceeding 350 words.

Drawings, diagrams or other illustrations should be made on larger scale (preferably) twice the size than the ones in which they are intended to appear. They should be done in Indian ink on bristol board with lettering in pencil. Scale of magnification of camera lucida tracings should be indicated by the side of drawings. In certain special cases arrangements will also be made for monochrome lithographic and other colour plates. Reduction of illustrations desired should be indicated in pencil. Appropriate legends should accompany all drawings. Names of authors are to be marked in pencil on the left-hand corner of drawing sheets. Photomicrographs should be securely mounted with colourless paste.

All tables, quotations and footnotes which will be set hereafter (beginning from Vol. I, No. 2) in types smaller than the text, should be typewritten on separate sheets and placed with the text in proper sequence. Footnotes should be numbered in Arabic numerals.

References to literature in the text should be given, whenever possible, in chronological order, only the names of authors and years of publication, in brackets, being given. They should be cited in full after the summary, the authors' names following in alphabetical order. Thus,

Name or Names of author; Name of Journal (abbreviation) with a single underline; Year of publication; Number of Volume with a double underline, and lastly page. The following would be a useful illustration:—

Bergmann and Stather . . . . . Z. Physiol. Chem., 1926, 152, 189.

Two copies of slip-proof and wherever possible, a page proof for final revision will be sent to authors. All corrections are best made on the slip-proof which should be transmitted to the Office of the Academy. All proof corrections involve heavy expenses which would be negligible if the papers are carefully revised by the authors before submission.

Fifty free reprints including plates and with cover will be supplied for each paper. Additional copies can be supplied at cost on previous intimation.

Blocks appearing in the *Proceedings* will be available for purchase by their respective authors. Orders for the same should be sent along with the corrected proofs and in any case not later than one month after the date of publication of the paper. The price charged would be 25% of the actual cost of the blocks *plus* freight and despatching charges. If the blocks are reproduced in other journals or publications, due acknowledgment should be made in them to the *Proceedings*.

The original drawings and plates of blocks appearing in the *Proceedings* will be returned to such of the authors as may require them provided the cost of despatching such originals is borne by them.

CONTENTS

PAGE

The Diffraction of Light by Two Superposed Parallel Supersonic Waves Being Harmonics of the Same Fundamental . . . . . Robert Mertens 289

Sum-Coincidence Technique for γ-Ray Studies . . . . . S. Jha, H. G. Devare, M. Narayana Rao and Kumari G. C. Pramila 303

The Dark Colour of Black Cotton Soils . . . . . V. S. Ramachandran, F. U. Ahmad and L. C. Jain 314

The Absorption and Fluorescence Spectra of Uranyl Nitrate Solutions at Room Temperature . . . . . D. D. Pant and D. P. Khandelwal 323

Studies on Metallic Halide Dioxanates. II. Dioxanates of Cupric and Ferric Chlorides . . . . . S. G. K. Nair and S. S. Moosath 336

Decay of Eu^{155} . . Kumari S. Y. Ambiye, M. C. Joshi and B. V. Thosar 342